

# Multiple dispersive bounds. II) Sub-threshold branch-cuts

Silvano Simula

*Istituto Nazionale di Fisica Nucleare, Sezione di Roma Tre,  
Via della Vasca Navale 84, I-00146 Rome, Italy*

Ludovico Vittorio

*Physics Department and INFN Sezione di Roma,  
Università di Roma La Sapienza, P.le A. Moro 2, I-00185 Roma, Italy*

We apply the general framework of multiple dispersive bounds, firstly discussed in the companion paper [1], to the study of sub-threshold branch-cuts. We propose the simultaneous application of a double dispersive bound as a proper way to take into account unitarity constraints within phenomenological analyses of hadronic form factors in the presence of sub-threshold branch-cuts. Accordingly, the standard  $z$ -expansion of hadronic form factors, commonly referred to as the Boyd-Grinstein-Lebed approach [2–5], is modified by including simultaneously the dispersive bounds related to the pair-production and to the sub-threshold regions. For the latter one the effects of above-threshold poles are described through a new resonance model and the possible choices of the outer function outside the pair-production region are discussed. A detailed numerical analysis of the experimental data or lattice QCD results in the spacelike region for the charged kaon form factor is presented as a direct application of the procedure of double dispersive bound. The comparison with other methodologies present in literature and with the  $z$ -expansion based on the single, total dispersive bound clearly shows that the  $z$ -expansion including the double dispersive bound provides the most precise extrapolation at large momentum transfer as well as the most stable results with respect to the choice of the outer function outside the pair-production region.

## I. INTRODUCTION

A proper treatment of sub-threshold branch-cuts through unitarity and analyticity is called for in the study of many physical processes, ranging from the analysis of the electromagnetic form factors to weak semileptonic decays of hadrons. Indeed, the hadronic form factors describing the transition induced by a current  $J$  between two hadrons  $H_1$  and  $H_2$ , may be characterized by a branch-cut starting below the pair-production threshold. Such *sub-threshold* cut corresponds to the production of on-shell particles  $\bar{H}_1' H_2'$  and to their subsequent scattering onto an off-shell pair  $\bar{H}_1 H_2$ .

In this work, we apply the general framework of multiple dispersive bounds, firstly discussed in the companion paper [1], to the study of sub-threshold branch-cuts within the standard  $z$ -expansion of hadronic form factors, commonly referred to as the Boyd-Grinstein-Lebed (BGL) approach [2–5]. Our goal is to implement the properties of unitarity and analyticity by imposing a double dispersive bound, which takes simultaneously into account unitarity in the pair-production region *and* within the lowest sub-threshold and the pair-production branch-points. We stress the importance of considering both constraints in the BGL  $z$ -expansion of hadronic form factors, at variance with what has been done till now in literature. In particular, while the first bound can be imposed through the knowledge of the so-called susceptibility, which can be estimated from the derivatives of appropriate two-point Green functions evaluated in momentum space, the second bound requires a separate estimate in a range of timelike values of the momentum transfer not accessible by experiments. To this end we develop a model for the effects of above-threshold resonances on the hadronic form factor. Our model successfully describes the  $\rho(770)$ -meson resonance in the case of the electromagnetic form factor of the pion, as well as the main poles entering the study of the electromagnetic form factors of charged and neutral kaons. Furthermore, we highlight that the choice of the outer function outside the pair-production arc is not unique and possible choices are discussed.

We analyze the experimental data [6, 7] or the lattice QCD (LQCD) [8] results available for the electromagnetic form factor of the charged kaon in the spacelike-region. The comparison with other methodologies present in literature and with the BGL  $z$ -expansion based on the single, total dispersive bound clearly shows that the  $z$ -expansion including the double dispersive bound provides the most precise extrapolation at large momentum transfer as well as the most stable results with respect to the choice of the outer function outside the pair-production region.

This paper is organized as follows. In Section II we review the basic properties of sub-threshold cuts, showing how double dispersive bounds can be directly imposed in the BGL  $z$ -expansion of hadronic form factors and, then, we compare our proposal with other expansions present in literature. In Section III we develop a model to describe the impact of above-threshold resonances on the form factor. The model is successfully tested in the case of the  $\rho(770)$ -meson pole for the electromagnetic form factor of the pion. In Section IV we focus on the electromagnetic form factors of charged and neutral kaons, decomposed in terms of isovector and isoscalar contributions. We implement our resonance model to take into account the  $\rho(770)$ , the  $\omega(782)$  and the  $\phi(1020)$  mesons. In Section V we discuss the ambiguity in the definition of the outer function outside the pair-production area and we evaluate its impact on the unitarity bound related to the region outside the pair-production arc. Section VI contains a detailed numerical study of the charged kaon form factor based on spacelike experimental or LQCD data. Different methodologies to impose unitarity are compared and the main result is that the  $z$ -expansion implementing the double dispersive bound provides the most precise extrapolation at large values of the momentum transfer as well as the most stable results with respect to the choice of the outer function outside the pair-production region. In the same Section we highlight also the impact of the application of the unitarity filter on the given set of input data (discussed in the companion paper [1]) and we compare our model-independent findings for the charged kaon radius with the model-dependent estimates made in the last PDG review [9] and in Ref. [8]. Finally, our conclusions are summarized in Section VII, while the Appendices contain further insights on some theoretical aspects discussed in the main text.

## II. SUB-THRESHOLD BRANCH-CUTS

For sake of simplicity, let us consider the case of a single, generic form factor  $f(t)$ , where  $t$  is the four-momentum transfer, describing the transition induced by a current  $J$  between two hadrons  $H_1$  and  $H_2$  with masses  $m_1$  and  $m_2$ , respectively.

As well known (see, e.g., Ref. [10]), unitarity implies that the form factor  $f(t)$  is an analytic function in the complex  $t$ -plane cut on the real axis from the lowest threshold  $t_{th}$  to infinity. When (isolated) real poles due to bound states are present below the threshold  $t_{th}$ , a product of appropriate Blaschke factors can be introduced to guarantee analyticity (see later on). The discontinuity across the cut is twice the imaginary part of  $f(t)$  along the cut and it is dictated by unitarity. The form factor  $f(t)$  is real for real values of  $t$  below  $t_{th}$ . The above analytical properties imply that the form factor  $f(t)$  may be represented through a dispersion relation of the form

$$f(t) = \frac{1}{\pi} \int_{t_{th}}^{\infty} dt' \frac{\text{Im}f(t')}{t' - t - i\epsilon} , \quad (1)$$

where the  $i\epsilon$  defines the integral for values of  $t$  on the branch-cut. Subtractions may be required to make the integral in Eq. (1) convergent.

In this work, at variance with Ref. [1], we consider the case of a lowest branch-cut starting below the pair-production threshold

$$t_{th} < t_+ \equiv (m_1 + m_2)^2 . \quad (2)$$

This may occur when an intermediate on-shell state  $\overline{H}_1' H_2'$  can be produced and scatter into an off-shell pair  $\overline{H}_1 H_2$ . In such a case, though the kinematical region between  $t_{th}$  and  $t_+$  is not experimentally accessible, the imaginary part of the form factor  $f(t)$  is non-vanishing and still dictated by unitarity.

Let us introduce the conformal mapping defined in terms of the variable

$$z_+ = z_+(t; t_0) \equiv \frac{\sqrt{t_+ - t} - \sqrt{t_+ - t_0}}{\sqrt{t_+ - t} + \sqrt{t_+ - t_0}}, \quad (3)$$

where  $t_0 < t_+$  is an auxiliary variable, which fixes the value of  $t$  at which  $z_+(t_0; t_0) = 0$ . For real values of  $t$  up to the threshold  $t_+$  the conformal variable  $z_+$  is real. For  $t \leq t_+$  it ranges from  $z = -1$  at  $t = t_+$  to  $z = 1$  for  $t \rightarrow -\infty$ . For values of  $t$  above the threshold  $t_+$  we have to specify the principal value of the square root to distinguish the first and the second Riemann sheets. Our convention is described in Appendix A, so that the first (physical) Riemann sheet corresponds to values of the conformal variable  $z_+$  always inside the unit disk (i.e.,  $|z_+| < 1$ ), while in the second Riemann sheet the values of  $z_+$  lie always outside the unit disk (i.e.,  $|z_+| > 1$ ). On the branch-cut one has always  $|z_+| = 1$ .

In terms of the conformal variable  $z_+$ , given by Eq. (3), the form factor  $f(z_+)$  is not analytic of the real type<sup>1</sup> inside the unit disk, since it has an imaginary part for real values of  $z_+$  between  $z_+ = -1$  and  $z_+ = z_+^{th} \equiv z_+(t_{th}; t_0)$  with  $-1 < z_+^{th}$  (for  $t_0 \leq t_{th}$  one has  $-1 < z_+^{th} \leq 0$ ). Such an extra branch-cut is depicted in red in Fig. 1.

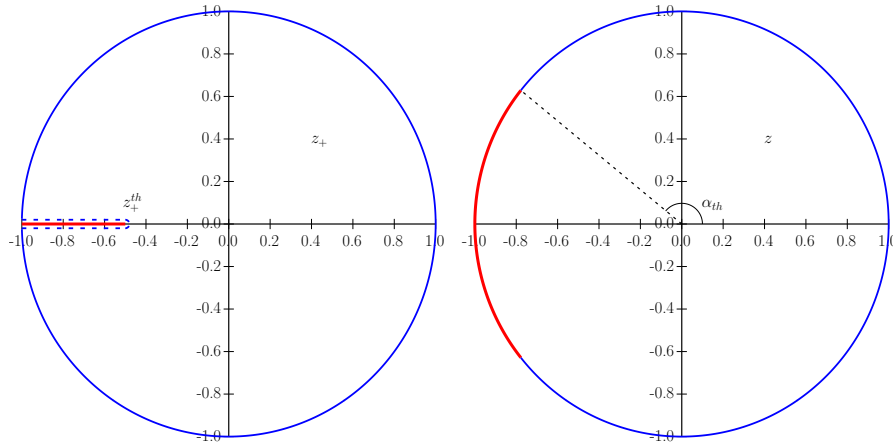


FIG. 1. Analytical domains in terms of the conformal variables  $z_+$  and  $z$ , given respectively by Eqs. (3) and (11) with  $t_{th} < t_+ = (m_1 + m_2)^2$ . The blue lines correspond to the pair-production branch-cut  $t \geq t_+$ , while the red ones to the extra branch-cut ranging from  $t_{th}$  to  $t_+$ . The lowest branch-point  $t_{th}$  is located at  $z_+^{th} = z_+(t_{th}; t_0)$  chosen arbitrarily to be equal to  $z_+^{th} = -0.5$ . Correspondingly, the angle  $\alpha_{th}$  is given by  $\cos(\alpha_{th}) = 2(1 + z_+^{th})^2 / (1 - z_+^{th})^2 - 1 \simeq -0.78$ .

### A. A model for the extra branch-cut

In Ref. [4] the issue of the possible presence of branch points inside the unit disk  $|z_+| < 1$  was addressed with the aim of providing a reasonable model for estimating the effects of the

<sup>1</sup> We remind that an analytic function is said to be of the real type when it satisfies the Schwarz reflection principle  $f(z_+^*) = f^*(z_+)$ , i.e. it is real on the real axis.

extra branch-cuts. The main assumption made in Ref. [4] is that extra branch-cuts arise from non-resonant processes with invariant masses below  $\sqrt{t_+}$ . Without loosing generality one can consider the case of a single extra branch-cut.

Let us indicate with  $f^{th}(z_+)$  the contribution of the single extra branch-cut, starting at  $t_{th} < t_+$ , to the form factor  $f(z_+)$ . For real values of  $z_+$  above  $z_+^{th}$  the function  $f^{th}(z_+)$  is real, while for  $z_+$  below  $z_+^{th}$  it acquires an imaginary part, which represents (half of) the discontinuity of the form factor  $f(z_+)$  along the extra branch-cut. Therefore, the difference  $f(z_+) - f^{th}(z_+)$  is an analytic function of the real type inside the unit disk  $|z_+| < 1$ , where it has a Taylor expansion with real coefficients. One gets

$$f(z_+) = f^{th}(z_+) + \frac{\sqrt{\tilde{\chi}}}{\phi_+(z_+)B_+(z_+)} \sum_{k=0}^{\infty} b_k z_+^k, \quad (4)$$

where  $\phi_+(z_+)$  is a kinematical function, analytic of the real type and without zeros inside the unit disk, while the quantity  $B_+(z_+)$  is a product of Blaschke factors related to (isolated) poles corresponding to bound states with masses  $M_R$  below the lowest threshold  $\sqrt{t_{th}}$ , namely

$$B_+(z_+) = \Pi_R \frac{z_+ - z_+^R}{1 - z_+ z_+^R} = \Pi_R z_+(t; M_R^2) \quad (5)$$

with  $z_+^R = z_+(M_R^2; t_0)$  being real and  $|z_+^R| < |z_+^{th}| < 1$ . The Blaschke product is unimodular on the unit circle (i.e.,  $|B_+(z_+)| = 1$  for  $|z_+| = 1$ ).

In Eq. (4)  $\tilde{\chi}$  is a *unitarity bound* on the difference  $f(z_+) - f^{th}(z_+)$ , so that the coefficients  $b_k$  should satisfy the unitarity constraint

$$\sum_{k=0}^{\infty} b_k^2 \leq 1. \quad (6)$$

In Ref. [4] it was argued that the quantity  $\tilde{\chi}$ , appearing in Eq. (4), can be replaced by its upper limit  $\tilde{\chi}^U$ , given by

$$\sqrt{\tilde{\chi}} \leq \sqrt{\tilde{\chi}^U} = \sqrt{\chi_+} + \sqrt{\chi_+^{th}} \quad (7)$$

with

$$\chi_+ \equiv \frac{1}{2\pi i} \oint_{|z_+|=1} \frac{dz_+}{z_+} |\phi_+(z_+)f(z_+)|^2, \quad (8)$$

$$\chi_+^{th} = \frac{1}{2\pi i} \oint_{|z_+|=1} \frac{dz_+}{z_+} |\phi_+(z_+)f^{th}(z_+)|^2. \quad (9)$$

In this work we choose the kinematical function  $\phi_+(z_+)$  to be the *outer function* adopted in the BGL approach of Refs. [2–5]. In this way it is possible to evaluate an upper limit to the quantity  $\chi_+$  from suitable two-point Green functions evaluated in momentum space (see Refs. [4, 11–15]), avoiding the explicit knowledge of the form factor  $f(z_+)$  on the unit circle.

According to Ref. [4] the term  $f^{th}(z_+)$  can be approximated by the smooth function

$$\begin{aligned}
 f^{th}(z_+) &= c \left[ \frac{\sqrt{(z_+ - z_+^{th})(1 - z_+ z_+^{th})}}{(1 - z_+)(1 - z_+^{th})} - \frac{1}{2} \frac{1 + z_+}{1 - z_+} \right] \\
 &= -\frac{c}{2} \frac{1 + z_+^{th}}{1 - z_+^{th}} \frac{\sqrt{1 - z_+^{th} z_+} - \sqrt{z_+ - z_+^{th}}}{\sqrt{1 - z_+^{th} z_+} + \sqrt{z_+ - z_+^{th}}} \\
 &= -\frac{c}{2} \frac{1 + z_+^{th}}{1 - z_+^{th}} \frac{(1 + z_+^{th})(1 - z_+)}{\left( \sqrt{1 - z_+^{th} z_+} + \sqrt{z_+ - z_+^{th}} \right)^2},
 \end{aligned} \tag{10}$$

where  $c$  is a coefficient incorporating the effects of the coupling of the current  $J$  with the external states  $\overline{H}_1 H_2$  through non-resonant on-shell intermediate states. In the r.h.s of Eq. (10) the subtraction of the second term guarantees that  $f^{th}(z_+)$  vanishes as  $z_+$  goes to 1 (i.e., when  $t \rightarrow \pm\infty$ ). Thus, once a reasonable estimate of the coefficient  $c$  has been established, one can use the model (10) to evaluate both the integral (9) and the difference  $f(z) - f^{th}(z)$  for a given set of known input data  $\{f_i\}$ , where  $f_i \equiv f[z_+(t_i; t_0)]$  with  $i = 1, 2, \dots, N$ . On such differences one can apply the expansion appearing in the r.h.s. of Eq. (4) with  $\tilde{\chi}$  replaced by  $\tilde{\chi}^U$  given in Eq. (7).

For sufficiently low values of  $c$  the impact of  $f^{th}(z_+)$  may be safely neglected. Such a situation may occur in specific cases, like, e.g., the one discussed in Ref. [4] concerning the impact of intermediate  $B_c^* + n\pi$  (with  $n$  a positive integer) states for  $B \rightarrow D$  and  $B \rightarrow D^*$  semileptonic decays. However, generally speaking, the model dependence of Eq. (10) may deteriorate the accuracy of the theoretical determinations of the input data  $\{f_i\}$ , coming, e.g., from lattice QCD (LQCD) simulations. Moreover, the model of Ref. [4] is based on the assumption that the extra cut arises only from non-resonant processes.

### B. The BGL expansion in terms of the conformal variable $z$

Instead of using the conformal variable  $z_+$  it is convenient to introduce the conformal variable  $z$  corresponding to the lowest branch-cut  $t_{th}$ , i.e.

$$z \equiv z_{th}(t; t_0) = \frac{\sqrt{t_{th} - t} - \sqrt{t_{th} - t_0}}{\sqrt{t_{th} - t} + \sqrt{t_{th} - t_0}} \tag{11}$$

with  $t_0 < t_{th} < t_+$ . In this way the unit circle  $|z| = 1$  corresponds to  $t \geq t_{th}$  and includes all the branch-cuts (see the right panel of Fig. 1).

In terms of the conformal variable  $z$  the BGL expansion of the form factor  $f(z)$  reads as

$$f(z) = \frac{\sqrt{\chi^U}}{\phi(z)B(z)} \sum_{k=0}^{\infty} a_k z^k, \tag{12}$$

where  $\phi(z)$  is a kinematical function to be specified, but analytic of the real type and without zeros inside the unit disk, while  $\chi^U$  is an *upper limit* to the quantity  $\chi[f]$ , associated to the form factor  $f(z)$  and defined as

$$\chi[f] \equiv \frac{1}{2\pi i} \oint_{|z|=1} \frac{dz}{z} |\phi(z)f(z)|^2 = \frac{1}{2\pi} \int_{-\pi}^{\pi} d\alpha |\phi(e^{i\alpha})f(e^{i\alpha})|^2 > 0, \tag{13}$$

namely

$$\chi[f] \leq \chi^U. \quad (14)$$

In Eq. (12) the quantity  $B(z)$  is the Blaschke factor removing the dynamical poles of the bound-states with invariant masses below  $\sqrt{t_{th}}$ , and it is an analytic function of the real type inside the unit  $z$ -disc. In terms of the conformal variable  $z$  one has<sup>2</sup>

$$B(z) = \Pi_R \frac{z - z^R}{1 - z z^R} = \Pi_R z_{th}(t; M_R^2), \quad (15)$$

where  $z^R = z_{th}(M_R^2; t_0)$  is real and  $|z^R| < 1$ . The Blaschke product is unimodular on the unit  $z$ -circle (i.e.,  $|B(z)| = 1$  for  $|z| = 1$ ) and, therefore, it does not contribute to Eq. (13).

Since the monomials  $z^k$  are orthonormal when integrated on the unit  $z$ -circle, the inequality (14) implies that the BGL coefficients  $a_k$  must satisfy the unitarity constraint

$$\sum_{k=0}^{\infty} a_k^2 \leq 1. \quad (16)$$

The important point is that in the case of a lowest branch-cut below the pair-production threshold ( $t_{th} < t_+$ ) the bound  $\chi^U$  on the form factor  $f(z)$  is related to the integral (13) over the unit  $z$ -circle, i.e. along the full branch-cut  $t \geq t_{th}$ . This feature can be easily derived also within the Dispersive Matrix (DM) method of Ref. [16], originally proposed in Refs. [15, 17] and based on the evaluation of a determinant of suitable inner products.

Putting  $z = e^{i\alpha}$  along the unit circle,  $\chi[f]$  can be split into the sum of two contributions

$$\chi[f] = \chi_{\text{pair}}[f] + \chi_{\text{extra}}[f] \quad (17)$$

where the angle  $\alpha_{th}$  corresponds to  $e^{i\alpha_{th}} = z_{th}(t_+; t_0)$ , namely

$$\alpha_{th} = \text{Arccos} \left[ 1 - 2 \frac{t_{th} - t_0}{t_+ - t_0} \right]. \quad (18)$$

In Eq. (17) the first term,  $\chi_{\text{pair}}[f]$ , corresponds to the contribution of the pair-production arc  $-\alpha_{th} \leq \alpha \leq \alpha_{th}$ , viz.

$$\chi_{\text{pair}}[f] = \frac{1}{2\pi} \int_{-\alpha_{th}}^{\alpha_{th}} d\alpha |\phi(e^{i\alpha}) f(e^{i\alpha})|^2, \quad (19)$$

while the second term,  $\chi_{\text{extra}}[f]$ , arises from the integration regions  $\alpha_{th} \leq |\alpha| \leq \pi$  outside the pair-production arc, namely

$$\chi_{\text{extra}}[f] = \frac{1}{2\pi} \left\{ \int_{-\pi}^{-\alpha_{th}} + \int_{\alpha_{th}}^{\pi} \right\} d\alpha |\phi(e^{i\alpha}) f(e^{i\alpha})|^2. \quad (20)$$

Generally speaking, both terms,  $\chi_{\text{pair}}[f]$  and  $\chi_{\text{extra}}[f]$ , depend on the form factor  $f(z)$  and on the kinematical function  $\phi(z)$ . However, a convenient choice for the latter one is

$$\phi(z) = \sqrt{\frac{dz_+}{dz}} \phi_+(z_+), \quad (21)$$

---

<sup>2</sup> The Blaschke factors  $B(z)$  and  $B_+(z_+)$  share the same zeros (located at  $t = M_R^2$ ), but they are different, namely  $B(z) \neq B_+(z_+)$ . The ratio  $B_+(z_+)/B(z)$  is an analytic function of the real type inside the unit  $z$ -disk and it is unimodular on the pair-production arc corresponding to both  $|z| = 1$  and  $|z_+| = 1$  (see Fig. 1).

where (we remind) the kinematical function  $\phi_+(z_+)$  is the *outer function* adopted in the BGL approach. On the pair-production arc  $-\alpha_{th} \leq \alpha \leq \alpha_{th}$ , where both  $z = e^{i\alpha}$  and  $z_+ = e^{i\alpha_+}$  are unimodular, one has

$$\frac{d\alpha_+}{d\alpha} \rightarrow \frac{z}{z_+} \frac{dz_+}{dz} = \frac{1+z}{1-z} \frac{1-z_+}{1+z_+} \rightarrow \frac{\text{tg}(\alpha_+/2)}{\text{tg}(\alpha/2)} \geq 0, \quad (22)$$

so that  $(d\alpha_+/d\alpha)$  is real and positive. Then, it follows that

$$|\phi(e^{i\alpha})|^2 = \frac{d\alpha_+}{d\alpha} |\phi_+(e^{i\alpha_+})|^2 \quad (23)$$

and, consequently, one finally gets

$$\begin{aligned} \chi_{\text{pair}}[f] &= \frac{1}{2\pi} \int_{-\alpha_{th}}^{\alpha_{th}} d\alpha |\phi(e^{i\alpha})f(e^{i\alpha})|^2 \\ &= \frac{1}{2\pi} \int_{-\pi}^{\pi} d\alpha_+ |\phi_+(e^{i\alpha_+})f(e^{i\alpha_+})|^2 = \chi_+[f]. \end{aligned} \quad (24)$$

Thus, adopting the kinematical function (21) one has  $\chi[f] = \chi_+[f] + \chi_{\text{extra}}[f]$ , which implies  $\chi[f] > \chi_+[f]$ , since in general  $\chi_{\text{extra}}[f] > 0$ . Thus, it is not guaranteed that an upper limit  $\chi_+^U$ , known for the integral  $\chi_+[f]$  related to the pair-production arc only, may act also as an upper limit to the global  $\chi[f]$ . This is not surprising. Consider the bound  $\chi_+^U$  obtained from the susceptibility of a suitable vacuum polarization function. The latter one takes into account only intermediate on-shell states  $\overline{H}_1 H_2$ , while the additional contribution  $\chi_{\text{extra}}[f]$  arises from intermediate off-shell states  $\overline{H}_1' H_2$ , generated by rescattering processes from intermediate on-shell states  $\overline{H}_1' H_2'$  having squared mass higher than  $t_{th}$  but lower than the pair production threshold  $t_+$ .

We point out that outside the pair-production arc, i.e. for  $\alpha_{th} < |\alpha| \leq \pi$ , the choice (21) is not unique. Indeed, one can multiply the r.h.s. of Eq. (21) by any function, which becomes unimodular on the pair-production arc. While such a factor does not modify the relation  $\chi_{\text{pair}}[f] = \chi_+[f]$ , it may affect the contribution  $\chi_{\text{extra}}[f]$ . This point will be discussed later in Section V.

To summarize, the main result of this Section is that in the case of a lowest branch-cut lower than the pair-production threshold ( $t_{th} < t_+$ ) the dispersive bound on the form factor  $f(z)$  is related to the integral of  $|\phi(z)f(z)|$  over the full unit circle  $|z| = 1$ , i.e. over all the branch-cuts. The latter ones are not limited to the arc  $-\alpha_{th} \leq \alpha \leq \alpha_{th}$  corresponding only to the pair-production branch-cut, but an additional contribution, which cannot be related to any susceptibility of the vacuum polarization function, should be considered (see Section II A and, more recently, Ref. [18]). While the bound  $\chi_+^U$  to the quantity  $\chi_{\text{pair}}[f] = \chi_+[f]$  can be obtained directly from the susceptibility of a suitable vacuum polarization function, the estimate of an upper limit  $\chi_{\text{extra}}^U$  to the quantity  $\chi_{\text{extra}}[f]$  will be discussed later in Section III. Thus, the bound  $\chi^U$  to the global quantity  $\chi[f]$  can be written as

$$\chi^U = \chi_+^U + \chi_{\text{extra}}^U. \quad (25)$$

### C. Semi-inclusive dispersive bounds

The decomposition (17) of the global quantity  $\chi[f]$  contains more information than the global quantity itself, which by definition is an inclusive quantity. The two contributions  $\chi_{\text{pair}}[f]$  and  $\chi_{\text{extra}}[f]$  can be viewed as *semi-inclusive* quantities, related to different partial regions of the

unit circle in the conformal variable  $z$ . Instead of imposing only the single, global filter  $\chi[f] \leq \chi^U = \chi_+^U + \chi_{\text{extra}}^U$ , we can apply simultaneously the double filter

$$\chi_{\text{pair}}[f] \leq \chi_+^U, \quad (26)$$

$$\chi_{\text{extra}}[f] \leq \chi_{\text{extra}}^U. \quad (27)$$

This is a case of the multiple dispersive bounds discussed in Ref.[1]. We expect that the simultaneous application of a double dispersive bound<sup>3</sup> can be more constraining than the one related to the single, total dispersive bound  $\chi^U$ . If the two dispersive bounds (26)-(27) are simultaneously fulfilled, then the global filter  $\chi[f] \leq \chi^U$  is automatically satisfied.

As shown in Ref. [1], it is straightforward to apply multiple filters to the BGL expansion (12). In the case of the double filter (26)-(27) the coefficients  $a_k$  of Eq. (12) must satisfy simultaneously two constraints

$$\sum_{k,k'=0}^{\infty} a_{k'} U_{k'k}(\alpha_{th}) a_k \leq \frac{\chi_+^U}{\chi^U} \quad (28)$$

and

$$\sum_{k,k'=0}^{\infty} a_{k'} [\delta_{k'k} - U_{k'k}(\alpha_{th})] a_k \leq \frac{\chi_{\text{extra}}^U}{\chi^U}, \quad (29)$$

where the matrix  $U$  is given by

$$U_{k'k}(\alpha_{th}) \equiv \frac{1}{2\pi} \int_{-\alpha_{th}}^{\alpha_{th}} d\alpha e^{i(k-k')\alpha} = \frac{1}{\pi} \frac{\sin(k-k')\alpha_{th}}{k-k'}. \quad (30)$$

The two unitarity constraints (28)-(29) automatically imply that the coefficients  $a_k$  satisfy the total unitarity constraint (16).

When a set of input data  $\{f_i\}$ , where  $f_i \equiv f[z_i = z(t_i; t_0)]$  with  $i = 1, 2, \dots, N$ , is known, the usual procedure is to truncate the BGL expansion (12) at some order  $M$ , namely

$$f^{(M)}(z) = \frac{\sqrt{\chi^U}}{\phi(z)B(z)} \sum_{k=0}^M a_k^{(M)} z^k \quad (31)$$

where the coefficients  $a_k^{(M)}$  satisfy the truncated double bound

$$\sum_{k,k'=0}^M a_{k'}^{(M)} U_{k'k}(\alpha_{th}) a_k^{(M)} \leq \frac{\chi_+^U}{\chi^U}, \quad (32)$$

$$\sum_{k,k'=0}^M a_{k'}^{(M)} [\delta_{k'k} - U_{k'k}(\alpha_{th})] a_k^{(M)} \leq \frac{\chi_{\text{extra}}^U}{\chi^U}, \quad (33)$$

which imply the total bound

$$\sum_{k=0}^M [a_k^{(M)}]^2 \leq 1. \quad (34)$$

---

<sup>3</sup> In what follows we limit ourselves to the case of a double dispersive bound, since we deal with the simplest case of two branch-cuts. The generalization to the case of multiple dispersive bounds related to multiple branch-cuts is straightforward.



The coefficients  $a_k^{(M)}$  are typically obtained from a  $\chi^2$ -minimization procedure applied to the set of input data  $\{f_i\}$ . The two semi-inclusive dispersive bounds (32)-(33) can be easily imposed by adding appropriate penalty terms to the  $\chi^2$ -variable.

The use of a finite order  $M$  in the truncated expansion (31) arises the issue of truncation errors, which were firstly discussed in Refs. [4, 5]. There, an upper limit to the truncation error was obtained, assuming that the coefficients  $a_k^{(M)}$  coincide with the first  $(M+1)$  coefficients  $a_k$  of the untruncated BGL expansion (12). See for details Appendix B.

Numerical applications of the double filter (26)-(27) will be presented in the case of the charged kaon electromagnetic form factor in Section VI.

#### D. Differences with other expansions

Equations (12)-(16), properly derived in the previous subsection, are however at variance with those proposed in Refs. [19–21] and adopted also in Refs. [22, 23]. Indeed, in Ref. [21] the BGL  $z$ -expansion of the form factor  $f(z)$  is written in the form

$$f(z) = \frac{\sqrt{\chi_+^U}}{\phi(z)B(z)} \sum_{k=0}^{\infty} c_k p_k(z; \alpha_{th}) , \quad (35)$$

where  $\chi_+^U$  is the dispersive bound to the quantity  $\chi_{\text{pair}}[f] = \chi_+[f]$ ,  $p_k(z; \alpha_{th})$  is an orthonormal polynomial of degree  $k$  on the arc  $-\alpha_{th} \leq \alpha \leq \alpha_{th}$  (i.e., a (normalized) Szegő polynomial [24]), and the (real) coefficients  $c_k$  satisfy the unitarity constraint

$$\sum_{k=0}^{\infty} c_k^2 \leq 1 . \quad (36)$$

In terms of the monomials  $z^k$  the  $z$ -expansion (35) can be written as (see Appendix C)

$$f(z) = \frac{\sqrt{\chi_+^U}}{\phi(z)B(z)} \sum_{k=0}^{\infty} b_k z^k , \quad (37)$$

where the (real) coefficients  $b_k$  satisfy an off-diagonal unitarity constraint limited only to the pair-production arc, namely

$$\sum_{k,k'=0}^{\infty} b_{k'} U_{k'k}(\alpha_{th}) b_k \leq 1 . \quad (38)$$

In Section IIB we have shown that the proper global dispersive bound is given by Eq. (14), which is related to the full branch-cut starting from  $t_{th}$ . The form factor  $f(t)$  has an imaginary part not only for  $t \geq t_+$ , but also for  $t_{th} \leq t \leq t_+$ , and its structure for both branch-cuts is dictated by unitarity (see later Section IV). Consequently, the global dispersive bound  $\chi^U$  should include the effects of both branch-cuts, and it is not legitimate to split Eq. (25) into two contributions and consider only one of them (in particular, the contribution of the pair-production arc). Furthermore, in Appendix D it is shown that the matrix  $U$  acts basically as a projector. In the limit of large values of its dimension it has only two possible eigenvalues equal to either 0 or 1. Thus, the expansion (37) can be split into the sum of two contributions related respectively to the (orthogonal) subspaces of the eigenvectors of  $U$  corresponding to eigenvalues equal to 0 or 1. The constraint (38) bounds only the contribution living in the subspace of the eigenvectors of  $U$  corresponding to eigenvalues equal to 1, while the other contribution is left unbounded.

### III. THE CONTRIBUTION $\chi_{\text{extra}}[f]$ AND ITS DISPERSIVE BOUND $\chi_{\text{extra}}^U$

The main result of the previous Section is that the BGL expansion (12) can be straightforwardly applied to the case of a lowest threshold  $t_{th}$  below the pair production one  $t_+$  by using the conformal variable  $z$  defined in terms of the lowest branch-point  $t_{th}$ , i.e. Eq.(11). The dispersive bound is given by Eq. (25) and it receives contributions both from the pair-production branch-cut,  $\chi_{\text{pair}}^U$ , and from the extra branch-cut,  $\chi_{\text{extra}}^U$ . With a suitable choice of the outer function, i.e. Eq. (21), the former contribution can be expressed through the susceptibility calculable in terms of derivatives of an appropriate vacuum polarization function.

In this Section we want to address the issue of estimating the additional contribution  $\chi_{\text{extra}}^U$  arising from resonant processes with invariant masses above the threshold  $\sqrt{t_{th}}$ , but below the pair-production threshold  $\sqrt{t_+}$ .

It is however instructive to start with the different case in which no extra branch-cut is present, i.e.  $t_{th} = t_+$ , and to try to describe (at least qualitatively) the impact on the structure of the form factor  $f(t)$  induced by the presence of a resonance  $R$  with a mass  $M_R$  above the pair-production threshold  $\sqrt{t_+}$ .

#### A. Effects of above-threshold poles on the form factor $f(t)$

It is well known [25] that a pole in the scattering amplitude or in the S-matrix in the second Riemann sheet may induce a zero of the S-matrix at the corresponding point in the first Riemann sheet (the physical sheet). This property turns out to be quite useful for searching the location of resonances in scattering processes (see for instance Ref. [26]).

Let us consider besides the form factor  $f(t)$ , describing the transition induced by a current  $J$  between two hadrons  $H_1$  and  $H_2$  with masses  $m_1$  and  $m_2$ , also the elastic scattering amplitude  $h(t)$  (with the appropriate quantum numbers) between the two hadrons (see Refs. [10, 27, 28]). In the elastic region  $t_+ \leq t \leq t_{in}$ , where  $t_{in}$  is the first inelastic threshold, unitarity implies [25] that  $\text{Im}f(t) = \rho(t)h(t)f^*(t)$ , where  $\rho(t)$  is a simple phase space factor. A well-known consequence of this relation is the Fermi-Watson theorem [29, 30], stating that in the elastic region the phases of the form factor  $f(t)$  and of the scattering amplitude  $h(t)$  are the same. The analytic continuation of the form factor  $f(t)$  to the second Riemann sheet can be done by matching the lower edge of the branch-cut in the first sheet with the upper edge of the branch-cut in the second sheet, namely  $f^{II}(t + i\epsilon) = f^I(t - i\epsilon)$ . Thus, indicating for sake of simplicity all quantities without a superscript as defined in the first Riemann sheet, unitarity implies that  $f^{II}(t) = f(t)/S(t)$ , where  $S(t) = 1 + 2i\rho(t)h(t)$  is the S-matrix in the first sheet. Thus, assuming that  $f(t)$  does not vanish at the zeros of  $S(t)$ , the form factor  $f(t)$  has poles in the second Riemann sheet in the same location of the zeros of  $S(t)$  (or, equivalently, at the same location of the poles of the scattering amplitude  $h(t)$ ).

Let us now translate the above properties in terms of the conformal variable  $z_+$ . The conjugate poles due to the resonance  $R$  are located at  $t = t_R^\pm = (M_R \pm i\Gamma_R/2)^2$ , where  $\Gamma_R$  is the resonance width and  $M_R^2 > t_+$ . Thus, according to Eqs. (A1)-(A2) the above poles occur in the second Riemann sheet (i.e. for  $|z_+| > 1$ ) at  $z_+ = (z_R^\pm)^{II} = 1/z_R^\pm$  with

$$z_R^\pm = |z_R| e^{\pm i\alpha_R}, \quad (39)$$

$$|z_R| = \sqrt{z_R^- z_R^+} = \sqrt{\frac{r + t_+ - t_0 - \sqrt{2(t_+ - t_0)(r + x)}}{r + t_+ - t_0 + \sqrt{2(t_+ - t_0)(r + x)}}} < 1, \quad (40)$$

$$\cos\alpha_R = \frac{r - t_+ + t_0}{\sqrt{r^2 + (t_+ - t_0)^2 - 2(t_+ - t_0)x}}, \quad (41)$$

where

$$\begin{aligned} r &= \sqrt{x^2 + M_R^2 \Gamma_R^2}, \\ x &= t_+ + \frac{\Gamma_R^2}{4} - M_R^2. \end{aligned} \quad (42)$$

Thus, one might ask whether (and to what extent) the impact of the resonance  $R$  on the form factor  $f(z)$  can be approximated by the following simple Ansatz

$$\begin{aligned} f_R(z_+) &= f_R(0) \frac{(1 - z_+)^2}{(1 - z_R^- z_+)(1 - z_R^+ z_+)} \\ &= f_R(0) \frac{(1 - z_+)^2}{1 - 2|z_R| \cos \alpha_R z_+ + |z_R|^2 z_+^2}, \end{aligned} \quad (43)$$

where  $f_R(0) \equiv f_R(z_+ = 0)$  represents the value of the form factor at  $z_+ = 0$  (i.e. at  $t = t_0$ ) and the term  $(1 - z_+)^2$  in the numerator has been inserted in order to guarantee that  $f_R(z) \propto 1/(-t)$  at large values of  $|t|$ . In Eq. (43) the conjugate poles occur only in the second Riemann sheet ( $|z_+| > 1$ ) at  $z_+ = 1/z_R^\pm$ . The function  $f_R(z_+)$  is analytic of the real type inside the unit disk  $|z_+| < 1$  and requires only the knowledge of the mass  $M_R$  and width  $\Gamma_R$  of the resonance.

### B. The electromagnetic form factor of the charged pion

We now check the quality of the approximation (43) by considering the case of the electromagnetic form factor for charged pions,  $F_\pi^{(em)}(t)$ , which is known to receive a dominant contribution from the  $\rho(770)$ -meson resonance for  $|t| \lesssim 1 \text{ GeV}^2$  (see also the recent work of Ref. [31]). In this note we make use of the results of Ref. [32], based on a detailed analysis of a large set of both space-like ( $t < 0$ ) and time-like experimental data up to  $t = 1 \text{ GeV}^2$ , carried out within a dispersive approach satisfying unitarity and analyticity.

Since the pion form factor  $F_\pi^{(em)}(t)$  is related to the matrix element of a vector current, angular momentum conservation imposes a specific constraint at the threshold  $t_+ = 4M_\pi^2$ , namely, in terms of the conformal variable  $z_+$  one must have  $dF_\pi^{(em)}(z_+)/dz_+|_{z_+=-1} = 0$  (see Ref. [33]). Therefore, we modify Eq. (43) with  $R = \rho$  by including as extra factor  $(1 + b_1 z_+)$ , with  $b_1$  chosen to guarantee that  $df_\rho(z_+)/dz_+|_{z_+=-1} = 0$ . Moreover, charge conservation implies that  $F_\pi^{(em)}(t = 0) = 1$ , which can be easily implemented by choosing the auxiliary variable  $t_0$  in the definition of the conformal variable  $z_+$  equal to  $t_0 = 0$  and by putting  $f_\rho(z_+ = 0) = 1$ . One has

$$f_\rho(z_+) = \frac{(1 - z_+)^2}{1 - 2|z_\rho| \cos \alpha_\rho z_+ + |z_\rho|^2 z_+^2} (1 + b_1 z_+) \quad (44)$$

with<sup>4</sup>

$$b_1 = \frac{1}{2} \frac{1 - |z_\rho|^2}{1 + |z_\rho| \cos \alpha_\rho}. \quad (45)$$

---

<sup>4</sup> Explicitly one has  $b_1 \simeq 0.0398$  (in the general case  $0 < b_1 < 1$ ). Thus, the function (44) has a zero only at  $z_+ = 1$  on the unit circle.

In Fig. 2 we show the predictions of Eq. (44) for  $t \leq 1 \text{ GeV}^2$ , obtained adopting the values of the  $\rho$ -meson mass and width from the latest PDG review [9], namely  $M_\rho = 775 \text{ MeV}$  and  $\Gamma_\rho = 147 \text{ MeV}$ . The locations of the conjugate poles (39) correspond to  $|z_\rho| = 0.930$  and  $\alpha_\rho/\pi = 0.232$ . Such predictions are compared both with the dispersive results of Ref. [32] in the case of the absolute value of the pion form factor and directly with the experimental data on  $\pi - \pi$  scattering phase shifts from Refs. [34, 35].

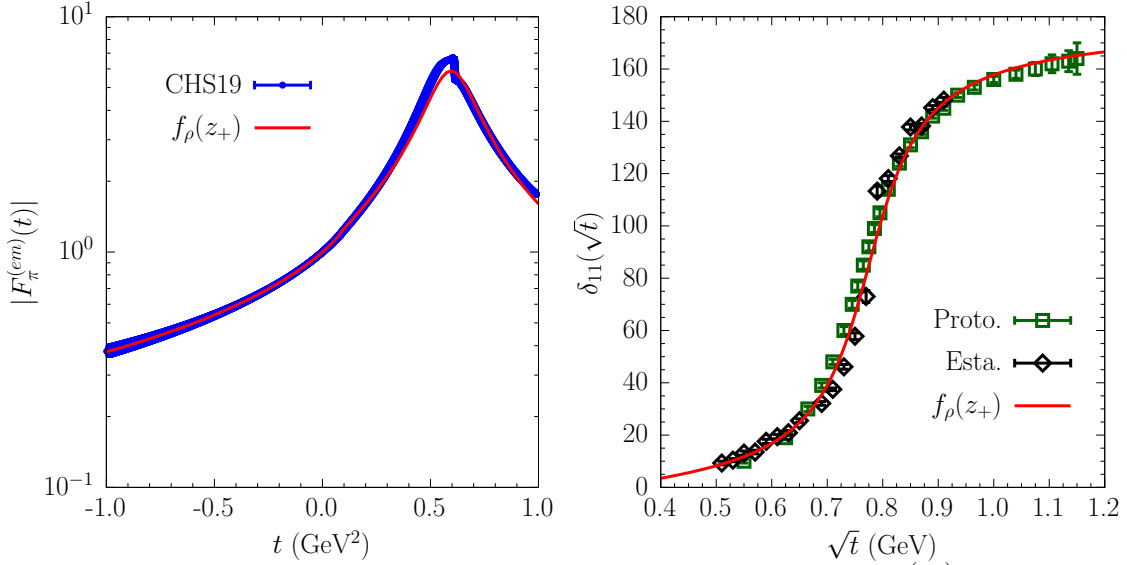


FIG. 2. Left panel: the absolute value of the electromagnetic pion form factor  $F_\pi^{(em)}(t)$ , determined by the dispersive analysis of experimental data made in Ref. [32], labelled as CHS19, compared with the corresponding predictions of the approximation (44), obtained using  $M_\rho = 775 \text{ MeV}$  and  $\Gamma_\rho = 147 \text{ MeV}$  from PDG [9]. Right panel: the experimental data on  $\pi - \pi$  scattering phase shifts from Ref. [34] (green squares) and Ref. [35] (black diamonds) compared with the phase of the form factor (44).

It can be seen that the approximation (44) works quite well almost everywhere for  $|t| \leq 1 \text{ GeV}^2$ . As a matter of fact, the differences with respect to the results of Ref. [32] are within the  $\simeq 5\%$  level except in the region around the  $\rho$ -meson peak, where they may reach the  $\simeq 15\%$  level. This is due to the fact that the analysis of Ref. [32] includes the effects of the  $\rho - \omega$  mixing, which is the most important isospin-breaking effect, enhanced around the peak by the small mass difference between the  $\rho$  and  $\omega$  resonances.

Finally, assuming  $F_\pi^{(em)}(z_+) = f_\rho(z_+)$  and adopting the kinematical function  $\phi_+(z_+)$  corresponding to the pion channel, i.e.  $\phi_+(z_+) = (1536\pi)^{-1/2} (1+z_+)^2 \sqrt{1-z_+}$  (see, e.g., Ref. [36]), we can evaluate directly the quantity  $\chi_+[f]$  given by Eq. (8). One gets  $\chi_+[F_\pi^{(em)} = f_\rho] \simeq 0.889\chi_+^U$ , where  $\chi_+^U = 0.00574$  is the dispersive bound obtained in Ref. [36] from lattice-based results of the light-quark vector susceptibility. In other words, almost 90% of the pion susceptibility  $\chi_+^U$  comes from the  $\rho$ -meson resonance.

### C. A modified $z$ -expansion to include effects from above-threshold poles

The above results indicate clearly that Eq. (43) is able to intercept the basic effects of an above-threshold resonance. In terms of the variable  $t$  one has

$$f_R(t) = f_R(t_0) \frac{1 + A}{1 - \frac{t-t_0}{r+t_+-t_0} + A\sqrt{\frac{t_+-t}{t_+-t_0}}} , \quad (46)$$

where the constant  $A$  is given by

$$A = \frac{\sqrt{2(t_+-t_0)(r+x)}}{r+t_+-t_0} \quad (47)$$

with  $r$  and  $x$  given by Eq. (42). Note that Eq. (46) differs from the Breit-Wigner parameterization for a resonant shape<sup>5</sup>. In the zero-width limit,  $\Gamma_R \rightarrow 0$ , one has  $(r+x) \rightarrow 0$  and  $(r+t_+) \rightarrow M_R^2$ , so that the function (46) (and correspondingly also Eq. (43)) reduces to the simple pole Ansatz

$$f_R(t) \xrightarrow{\Gamma_R \rightarrow 0} f_R(t_0) \frac{M_R^2 - t_0}{M_R^2 - t} . \quad (48)$$

Since  $f_R(z_+)$  is an analytic function of the real type inside the unit disk  $|z_+| < 1$ , an interesting development could be to modify the standard BGL  $z$ -expansion (12) or the Bourrely-Caprini-Lellouch (BCL)  $z$ -expansion [33] by taking into account an above-threshold resonance through the function (43).

In the BGL case<sup>6</sup> one has

$$f(z_+) = f_R(z_+) \frac{\sqrt{\chi_+^U}}{\phi_+(z_+)B_+(z_+)} \sum_{k=0}^{\infty} b_k z_+^k , \quad (49)$$

where the (real) coefficients  $b_k$  satisfy the off-diagonal unitarity constraint

$$\sum_{k,k'=0}^{\infty} b_{k'} \mathcal{S}_{k'k} b_k \leq 1 \quad (50)$$

with

$$\mathcal{S}_{k'k} \equiv \frac{1}{2\pi i} \oint_{|z_+|=1} \frac{dz_+}{z_+} |f_R(z_+)|^2 z_+^{*k'} z_+^k = \frac{1}{2\pi} \int_{-\pi}^{\pi} d\alpha_+ |f_R(e^{i\alpha_+})|^2 e^{i(k-k')\alpha_+} . \quad (51)$$

Following the simple procedure described in Appendix C, the  $z$ -expansion (49) can be rewritten in the form

$$f(z_+) = f_R(z_+) \frac{\sqrt{\chi_+^U}}{B_+(z_+)} \sum_{k=0}^{\infty} a_k s_k(z_+) , \quad (52)$$

<sup>5</sup> It is straightforward to check that: i) for real values of  $t$  Eq. (46) has an imaginary part only for  $t > t_+$ , and ii) taking the principal value of  $\sqrt{t_+-t}$  (see Eq. (A1)), Eq. (46) has no pole in the complex  $t$ -plane.

<sup>6</sup> A modified BCL-like  $z$ -expansion can be obtained simply by omitting the function  $\sqrt{\chi_+^U}/\phi_+(z_+)$  in Eq. (49) and by multiplying the integrand of Eq. (51) by  $|\phi_+(z_+)|^2/\chi_+^U$ .

where  $s_k(z_+) = \sum_{m=0}^k L_{km}^{-1} z_+^m$  is a polynomial<sup>7</sup> of degree  $k$ , obtained from the inverse of the lower triangular matrix of the Cholesky decomposition of the matrix  $\mathcal{S} = LL^T$ , and the (real) coefficients  $a_k$  satisfy the diagonal unitarity constraint

$$\sum_{k=0}^{\infty} a_k^2 \leq 1 . \quad (53)$$

Summarizing, by means of the function (43) the  $z$ -expansion (49) can be constructed to include the main effects of an above-threshold resonance. This is at variance with the simple pole Ansatz (48), which does not possess the correct analytical properties in the unit disk. At most, for narrow resonances ( $\Gamma_R/M_R \ll 1$ ) the pole Ansatz may work as an approximation of the function (43) in the kinematical region  $t \lesssim t_+$ , but not in the timelike one  $t > t_+$  (particularly, when  $t \approx M_R^2$ )<sup>8</sup>.

Numerical applications of the  $z$ -expansion (49), or equivalently Eq. (52), to phenomenological cases of interest are beyond the aim of the present work.

#### IV. THE ELECTROMAGNETIC FORM FACTOR OF THE CHARGED KAON

Let us now address the issue of the presence of an extra branch-cut located at  $t_{th}$  generated by resonant processes with invariant masses below the pair-production threshold  $t_+$ . To this end we focus on the case of the electromagnetic form factors of charged and neutral kaon mesons.

In the kaon case, while the pair-production threshold is located at  $t_+ \equiv t_{2K} = 4m_K^2 \simeq 0.98$  GeV<sup>2</sup>, an extra branch-cut starts at the pion production threshold  $t_{th} \equiv t_{2\pi} = 4m_\pi^2 \simeq 0.08$  GeV<sup>2</sup>. In the kinematical region between  $t_{2\pi}$  and  $t_{2K}$ , which is not accessible directly in timelike  $e^+e^- \rightarrow \bar{K}K$  processes, the dominant reaction mechanism is expected to proceed via  $\pi\pi$  (on-shell) intermediate states that scatter inelastically into the final pair of (off-shell) kaons. Such scattering is expected to be governed mainly by the presence of  $\rho$ - and  $\omega$ -meson resonances.

We now basically refer to the dispersive analysis made in Ref. [37]. The electromagnetic form factors of charged and neutral kaons,  $F_{K^\pm}^{(em)}(t)$  and  $F_{K^0}^{(em)}(t)$ , can be decomposed into an isovector (V) and an isoscalar (S) contributions

$$F_{K^\pm}^{(em)}(t) = F_K^{(S)}(t) + F_K^{(V)}(t) , \quad (54)$$

$$F_{K^0}^{(em)}(t) = F_K^{(S)}(t) - F_K^{(V)}(t) , \quad (55)$$

where the isovector part has the lowest branch point at  $t_{2\pi} = 4m_\pi^2$ , while for the isoscalar part the lowest branch-cut starts at  $t_{3\pi} = 9m_\pi^2$ . Charge conservation implies that  $F_K^{(V)}(0) = F_K^{(S)}(0) = 1/2$ . For the isovector component  $F_K^{(V)}(t)$  unitarity implies [38]

$$\text{Im} F_K^{(V)}(t) = \frac{t}{4\sqrt{2}} \left(1 - \frac{t_{2\pi}}{t}\right)^{3/2} [g_1^1(t)]^* F_\pi^{(em)}(t) \Theta(t - t_{2\pi}) , \quad (56)$$

<sup>7</sup> The polynomials  $s_k(z_+)$  are an orthonormal set on the unit circle  $|z_+| = 1$  with respect to a weight function given by  $|f_R(z_+)|^2$ , namely

$$\frac{1}{2\pi i} \oint_{|z_+|=1} \frac{dz_+}{z_+} |f_R(z_+)|^2 s_k(z_+) s_{k'}^*(z_+) = \delta_{kk'} .$$

<sup>8</sup> At first order in  $\Gamma_R/M_R$  one has

$$f_R(t) \simeq f_R(t_0)(M_R^2 - t_0 + \tilde{\Gamma}_R \sqrt{t_+ - t_0}) / (M_R^2 - t + \tilde{\Gamma}_R \sqrt{t_+ - t})$$

with  $\tilde{\Gamma}_R = \Gamma_R \sqrt{(M_R^2 + t_+)/2(M_R^2 - t_+)}$ .

where  $F_\pi^{(em)}(t)$  is the timelike pion form factor, described in Section III B, and  $g_1^1(t)$  represents the p-wave component of the angular decomposition of the  $\pi\pi \rightarrow \bar{K}K$  scattering amplitude. Both  $F_\pi^{(em)}(t)$  and  $g_1^1(t)$  satisfy dispersion relations with a branch-cut starting at  $t_{th} = t_{2\pi}$  (see, e.g., Ref. [39]).

Data on the phase and modulus of  $g_1^1(t)$  are available in the physical region  $t \geq t_{2K}$  from  $\pi\pi \rightarrow \bar{K}K$  scattering. Instead, in the unphysical region  $t_{2\pi} \leq t \leq t_{2K}$  such data cannot occur. However, thanks to Eq. (56) the phase of  $g_1^1(t)$  must compensate the one of the pion form factor, which in turn for  $t \leq t_{2K} \sim 1 \text{ GeV}^2$  is dominated by the phase of the elastic  $\pi\pi$  scattering. Since the phase of  $g_1^1(t)$  is known for  $t \geq t_{2\pi}$ , then its modulus can be reconstructed [39] using the standard Muskhelishvili-Omnès method [40, 41]. Using dispersive parameterizations of  $g_1^1(t)$ , elaborated in Ref. [39], and of the pion form factor  $F_\pi^{(em)}(t)$  (similar to the one developed in Ref. [32]), the isovector part of the kaon form factor  $F_K^{(V)}(t)$  was determined in Ref. [37] for  $t \geq t_{2\pi}$  and tested successfully against experimental data on  $\tau^- \rightarrow K^- K_S \nu_\tau$  decays [42] for  $t \geq t_{2K}$ . It turned out that  $F_K^{(V)}(t)$  receives an important contribution from the  $\rho(770)$ -meson resonance and to a lesser extent from the  $\rho'(1450)$ -meson resonance.

As for the isoscalar part, the authors of Ref. [37] developed a model based on Breit-Wigner ansätze corresponding to the lowest-lying isoscalar vector resonances. The free parameters of the model were obtained by fitting several sets of cross-section data on the timelike reactions  $e^+e^- \rightarrow K^+K^-$  and  $e^+e^- \rightarrow K_S K_L$  (see for details Ref. [37]) as well as available spacelike data for electron scattering on charged kaons from FNAL [6] and CERN [7]. It turned out that  $F_K^{(S)}(t)$  receives contributions from the  $\omega(782)$ -meson resonance in the unphysical region below  $t_{2K}$  and from the  $\phi(1020)$ -meson resonance (and to a lesser extent from the  $\omega(1420)$ -meson resonance) in the physical region above  $t_{2K}$ .

The results for  $F_{K^\pm}^{(em)}(t)$  and  $F_{K^0}^{(em)}(t)$  obtained by the dispersive analysis of Ref. [37] are shown in Fig. 3 as the dotted blue lines for  $-1 \leq t(\text{GeV}^2) \leq 1.2$ , i.e. both in the spacelike region ( $t \leq 0$ ) and in the timelike one ( $t > 0$ ). Note that the uncertainties on both kaon form factors are available only in the spacelike region. The results of Ref. [37] are compared with the predictions based on our simple model (43) for above-threshold resonances. More precisely, we consider<sup>9</sup>

$$F_{K^\pm}^{(em)}(t) = \frac{1}{6}f_\omega(z_{3\pi}) + \frac{1}{3}f_\phi(z_{2K}) + \frac{1}{2}f_\rho(z_{2\pi}), \quad (57)$$

$$F_{K^0}^{(em)}(t) = \frac{1}{6}f_\omega(z_{3\pi}) + \frac{1}{3}f_\phi(z_{2K}) - \frac{1}{2}f_\rho(z_{2\pi}), \quad (58)$$

where  $f_\rho$  is given as in Eq. (44) and similarly for  $f_\omega$  and  $f_\phi$ . For each of the three resonances we adopt the conformal variable corresponding to the appropriate threshold, i.e.  $z_{2\pi}$ ,  $z_{3\pi}$  and  $z_{2K}$  corresponding respectively to the two-pion,  $t_{2\pi} = 4m_\pi^2$ , three-pion,  $t_{3\pi} = 9m_\pi^2$  and two-kaon,  $t_{2K} = 4m_K^2$ , thresholds. The auxiliary variable  $t_0$  is always chosen to be equal to  $t_0 = 0$  in order to easily ensure charge conservation at  $t = 0$ . Explicitly one has

$$z_k = \frac{\sqrt{t_k - t} - \sqrt{t_k}}{\sqrt{t_k - t} + \sqrt{t_k}} \quad (59)$$

with  $k = \{2\pi, 3\pi, 2K\}$ .

The predictions of Eqs. (57)-(58), using for the resonance parameters the PDG values [9], namely  $M_\rho = 775 \text{ MeV}$ ,  $\Gamma_\rho = 147 \text{ MeV}$ ,  $M_\omega = 782.7 \text{ MeV}$ ,  $\Gamma_\omega = 8.68 \text{ MeV}$ ,  $M_\phi = 1019.5$

<sup>9</sup> We take into account that the electromagnetic current for  $u$ -,  $d$ - and  $s$ -quarks is given by the sum of an isovector  $(\bar{u}\gamma^\mu u - \bar{d}\gamma^\mu d)/2$  and an isoscalar part  $(\bar{u}\gamma^\mu u + \bar{d}\gamma^\mu d - 2\bar{s}\gamma^\mu s)/6$ . We neglect any mixing between the light and the strange sectors for the lowest-lying vector resonances and we ignore isospin-breaking effects.

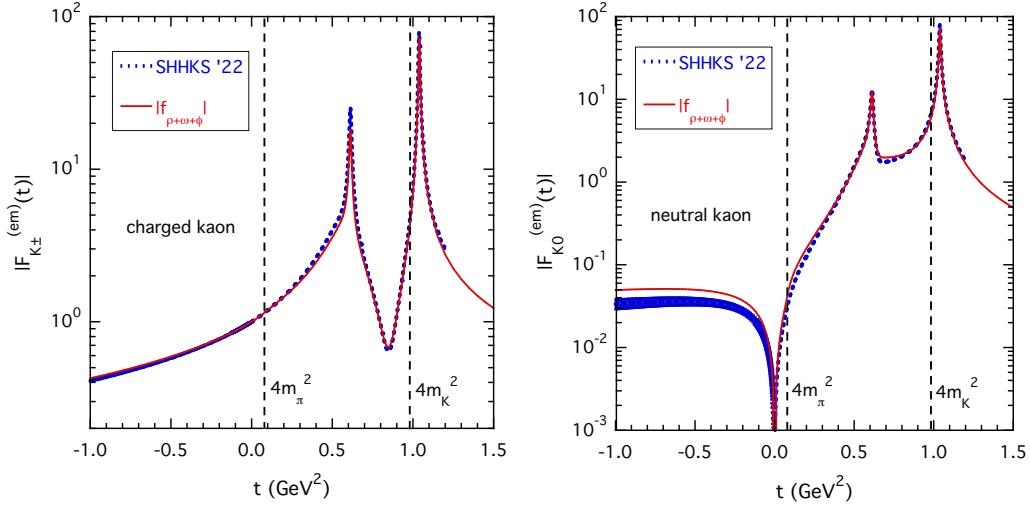


FIG. 3. Absolute value of the electromagnetic form factors of charged (left panel) and neutral kaons (right panel) versus the squared momentum transfer  $t$  both in the spacelike region ( $t \leq 0$ ) and in the timelike one ( $t > 0$ ). Dotted blue lines represent the results of the dispersive analysis of Ref. [37], labelled as SHHKS '22, while the solid red lines correspond to the predictions of the resonance model given by Eqs. (57)-(58) using the values  $M_\rho = 775$  MeV,  $\Gamma_\rho = 147$  MeV,  $M_\omega = 782.7$  MeV,  $\Gamma_\omega = 8.68$  MeV,  $M_\phi = 1019.5$  MeV and  $\Gamma_\phi = 4.25$  MeV taken from the PDG [9].

MeV and  $\Gamma_\phi = 4.25$  MeV, are shown in Fig. 3 by the solid red lines. The comparison with the dispersive results of Ref. [37] shows that the overall structure of both charged and neutral kaon form factors is reasonably reproduced for both timelike and spacelike values of  $t$ . In the pair-production region  $t \geq t_{2K} \simeq 1$  GeV<sup>2</sup> the differences are within  $\simeq 20\%$ , while they may reach  $\simeq 30\%$  in the unphysical region around the  $\rho(770)$ - $\omega(782)$  peaks for the case of the charged kaon. According to Ref. [37] that region is affected by SU(2)-breaking effects, which are not included in the simple resonance model of Eqs. (57)-(58).

Thus, the above findings suggest that a phenomenological estimate of the contribution  $\chi_{\text{extra}}^U$  to the dispersive bound  $\chi^U$  may be obtained using for the form factor a simple resonance model, based on the  $z$ -dependence of Eq. (43), for evaluating the integral (20) involving the product  $|\phi(z)f(z)|^2$  over the unphysical region  $\alpha_{th} \leq |\alpha| \leq \pi$  outside the pair-production arc (i.e.,  $t_{th} \leq t \leq t_+$ ). In the next Section we discuss the possible choices of the kinematical function  $\phi(z)$  outside the pair-production arc.

## V. THE OUTER FUNCTION $\phi(z)$ OUTSIDE THE PAIR-PRODUCTION ARC

As already observed in Section II B, a convenient choice for the kinematical function  $\phi(z)$  is provided by Eq. (21), namely

$$\phi(z) = \sqrt{\frac{dz_+}{dz}} \phi_+(z_+) = \sqrt{\frac{1+z}{1-z} \frac{1-z_+}{1+z_+} \frac{z_+}{z}} \phi_+(z_+), \quad (60)$$

where the function  $\phi_+(z_+)$  is the *outer function* adopted in the BGL approach [2–5] to describe the momentum dependence of the form factors relevant for the semileptonic weak decays of hadrons [5, 43] (see Appendix A of the companion paper [1] for the case of semileptonic decays of pseudoscalar mesons). In this way, for obtaining an upper limit to the contribution  $\chi_+^U$  inside the



pair-production arc one can make use of the susceptibility  $\chi_n$ , related to the appropriate derivative of the vacuum polarization function and calculable non-perturbatively on the lattice (see Refs. [16, 44–47]). We stress that this can be done without any knowledge of the  $z$ -dependence of the form factor on the pair-production arc.

However, outside the pair-production arc the choice of  $\phi(z)$  is not unique. Using the same auxiliary variable  $t_0$  for both conformal variables  $z_+$  and  $z$ , given respectively in Eqs. (3) and (11) with  $t_0 < t_{th} < t_+$ , the kinematical function  $\phi(z)$  may be chosen as

$$\phi(z) \equiv \sqrt{\left(\frac{z}{z_+}\right)^p \frac{dz_+}{dz} \phi_+(z_+)} , \quad (61)$$

where  $p$  is a generic constant. In this way, on the pair-production arc  $-\alpha_{th} \leq \alpha \leq \alpha_{th}$ , where both  $z_+$  and  $z$  are unimodular, Eq. (23) is still valid for any value of  $p$ , namely one has  $|\phi(e^{i\alpha})|^2 = (d\alpha_+/d\alpha) |\phi_+(e^{i\alpha_+})|^2$ . However, the value of  $p$  can be fixed by requiring that the integral  $\chi[f]$ , given by Eq. (13), is independent of the auxiliary variable  $t_0$ . This can be achieved by imposing that  $\phi(z)\sqrt{1-z^2}$  is independent of  $t_0$  (see the Appendix A of Ref. [36]). Since the product  $\phi_+(z_+)\sqrt{1-z_+^2}$  does not depend on  $t_0$  (by applying the independence of  $\chi_+[f]$  on  $t_0$ ), we have simply to impose that the quantity

$$\left(\frac{z}{z_+}\right)^p \frac{dz_+}{dz} \frac{1-z^2}{1-z_+^2} = \left(\frac{1+z}{1+z_+}\right)^2 \left(\frac{z}{z_+}\right)^{p-1} \quad (62)$$

is independent of  $t_0$ . Explicitly one gets

$$\left(\frac{1+z}{1+z_+}\right)^2 \left(\frac{z}{z_+}\right)^{p-1} = \frac{t_{th}-t}{t_+-t} \left(\frac{\sqrt{t_+-t} + \sqrt{t_+-t_0}}{\sqrt{t_{th}-t} + \sqrt{t_{th}-t_0}}\right)^{2p} , \quad (63)$$

so that Eq. (62) is independent of  $t_0$  only when  $p = 0$ .

Nevertheless, it is worth highlighting that also Eq. (61) does not represent the most general form for the kinematical function  $\phi(z)$ . Indeed, we can still multiply Eq. (61) by any function of  $z_+$  and  $z$ , which is analytic of the real type inside the unit disk  $|z| < 1$  and unimodular in the unit circle  $|z| = 1$ . Possible functions of this type are generic powers of specific ratios of the conformal variables corresponding to a fixed value of  $t_0 < t_{th}$ , namely  $z_+(t; 0)/z_{th}(t; 0)$  and  $z_+(t; t_-)/z_{th}(t; t_-)$ , which are clearly unimodular on the pair-production arc<sup>10</sup>. The conformal variables  $z_+(t; 0)$  and  $z_+(t; t_-)$  come into play [43] when suitable unimodular substitutions are used to extend the kinematical function known along the unit circle inside the unit disk. In the case of  $\phi_+(z_+)$  the following unimodular substitutions are adopted (see, e.g., Ref. [1])

$$\begin{aligned} \sqrt{t} &\rightarrow \sqrt{\frac{-t}{z(t; 0)}} = \sqrt{t_+-t} + \sqrt{t_+} , \\ \sqrt{t_- - t} &\rightarrow \sqrt{\frac{t_- - t}{z(t; t_-)}} = \sqrt{t_+-t} + \sqrt{t_+ - t_-} , \end{aligned} \quad (64)$$

where  $t_- \equiv (m_1 - m_2)^2$ . The above relations guarantee the analyticity and the absence of zeros of the function  $\phi_+(z_+)$  inside the unit disk  $|z_+| < 1$ . In the case at hand, an alternative choice is

---

<sup>10</sup> Any conformal variable  $z_+(t; t_0)$  (or  $z(t; t_0)$ ) becomes unimodular when  $t > t_+$  (or  $t > t_{th}$ ) regardless the value of  $t_0$ .

to use the conformal variables  $z(t; 0)$  and  $z(t; t_-)$ , so that the analyticity and the absence of zeros of the kinematical function  $\phi(z)$  inside the unit disk  $|z| < 1$  is always guaranteed. In other words, once  $\phi_+(z_+)$  is specified, several choices of the outer function  $\phi(z)$  are still possible outside the pair-production arc. For instance, in the unit disk the outer function  $\phi(z)$  can be written as:

$$\phi^{q_1 q_2}(z) = \sqrt{\frac{dz_+}{dz} \left[ \frac{z(t; 0)}{z_+(t; 0)} \right]^{q_1} \left[ \frac{z(t; t_-)}{z_+(t; t_-)} \right]^{q_2}} \phi_+(z_+), \quad (65)$$

where  $q_1$  and  $q_2$  are real powers. Explicitly, one has

$$\sqrt{\frac{z(t; 0)}{z_+(t; 0)}} = \frac{\sqrt{t_+ - t} + \sqrt{t_+}}{\sqrt{t_{th} - t} + \sqrt{t_{th}}} \quad \text{and} \quad \sqrt{\frac{z(t; t_-)}{z_+(t; t_-)}} = \frac{\sqrt{t_+ - t} + \sqrt{t_+ - t_-}}{\sqrt{t_{th} - t} + \sqrt{t_{th} - t_-}}.$$

The kinematical function  $\phi^{q_1 q_2}(z)$  is a legitimate outer function for any values of  $q_1$  and  $q_2$ , since inside the unit disk  $|z| < 1$  it fulfills the relation

$$\log \phi^{q_1 q_2}(z) = \frac{1}{2\pi} \int_{-\pi}^{\pi} d\alpha \frac{e^{i\alpha} + z}{e^{i\alpha} - z} \log |\phi^{q_1 q_2}(e^{i\alpha})|, \quad (66)$$

as it can be directly checked numerically.

One has  $|\phi^{q_1 q_2}(z)| = |\phi^{00}(z)| = |\phi(z)|$  when  $|z_+| = 1$ , which implies also  $|z| = 1$ . Therefore, the contribution  $\chi_+[f]$  on the pair-production arc is independent of the powers  $q_1$  and  $q_2$  and it can be always bounded by the appropriate susceptibility  $\chi_+^U = \chi_n$ . On the contrary, the contribution  $\chi_{\text{extra}}[f]$  outside the pair-production arc does depend on the powers  $q_1$  and  $q_2$ .

The choice (65) has been adopted in Ref. [21] for  $\Lambda_b \rightarrow \Lambda$  transition and in Ref. [23] for the  $B_s \rightarrow K$  form factors with specific choices of the powers  $q_1$  and  $q_2$ . In the case of the  $B_s \rightarrow K$  form factors [23] the powers  $q_1$  and  $q_2$  are equal to  $q_1 = 5$  and  $q_2 = -3/2$  for the vector form factor  $f_+$ , while  $q_1 = 4$  and  $q_2 = -1/2$  for the scalar form factor  $f_0$ . The corresponding  $t$ -dependencies of the kinematical functions (65) of the vector and scalar form factors for the  $B_s \rightarrow K$  transition are shown in the left panel of Fig. 4, where they are compared with those related to the choice  $q_1 = q_2 = 0$ . The differences are limited, particularly in the semileptonic decay region  $0 \leq t \leq t_- = (M_{B_s} - m_K)^2$ .

In the right panel of Fig. 4 an analogous comparison is made in the case of the electromagnetic form factor of the charged kaon. In this case, instead, large differences, even by orders of magnitude, are visible in the unphysical region  $t_{2\pi} \leq t \leq t_{2K}$ , particularly close to the lowest branch-point  $t_{2\pi}$ , and also for spacelike values of  $t$ . Since in this case  $t_0 = t_- = 0$  one has explicitly ( $q_1 + q_2 = 7/2$ )

$$|\phi^{q_1 q_2}(z)| \xrightarrow{q_1=5, q_2=-3/2} \sqrt{\left| \frac{z}{z_+} \right|^{7/2}} |\phi^{00}(z)| = \left| \frac{\sqrt{t_{2K} - t} + \sqrt{t_{2K}}}{\sqrt{t_{2\pi} - t} + \sqrt{t_{2\pi}}} \right|^{7/2} |\phi^{00}(t)|. \quad (67)$$

In the kaon case we have calculated the quantity  $4m_K^2 \chi_{\text{extra}}[f]$ , given by Eq. (20) with  $\alpha_{th}/\pi = 0.1823$ , adopting for the form factor either the dispersive results of Ref. [37] or the resonance model given by Eqs. (57)-(58), developed in the previous Section. We remind that in the timelike region the uncertainties of the kaon form factors of Ref. [37] are not available (a rough estimate indicates errors of the order of 10%). The results corresponding to the kinematical function  $\phi^{q_1 q_2}(z)$  (with  $\phi_+(z_+) = (1536\pi)^{-1/2} (1 + z_+)^2 \sqrt{1 - z_+}$ ) are collected in Table I for various values of  $q \equiv q_1 + q_2$ . The simple resonance model given by Eqs. (57)-(58) works quite well in the neutral kaon channel with respect to the results corresponding to the dispersive approach of Ref. [37] with differences well below the 10% level at any value of  $q$ . Instead, in the charged

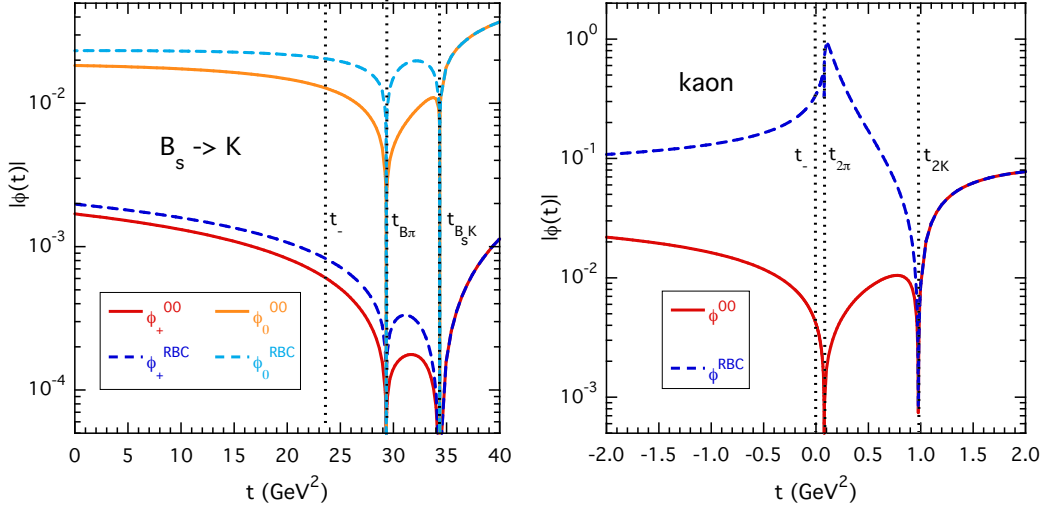


FIG. 4. Absolute values of the kinematical function (65) versus the squared 4-momentum transfer  $t$  corresponding to  $q_1 = q_2 = 0$  (solid lines) and to the choice of  $q_1$  and  $q_2$  made in Ref. [23] (dashed lines) and labelled with the suffix RBC (see text). The value of the auxiliary variable  $t_0$  is chosen to be equal to  $t_0 = t_-$ . Left panel: vector and scalar kinematical functions for the  $B_s \rightarrow K$  transition with  $t_- = (m_{B_s} - m_K)^2 \simeq 23.7 \text{ GeV}^2$ ,  $t_{th} = t_{B\pi} = (m_B + m_\pi)^2 \simeq 29.3 \text{ GeV}^2$  and  $t_+ = t_{B_s K} = (m_{B_s} + m_K)^2 \simeq 34.4 \text{ GeV}^2$ . Right panel: vector kinematical function corresponding to the case of the electromagnetic form factor of the charged kaon with  $t_- = 0$ ,  $t_{th} = t_{2\pi} = 4m_\pi^2 \simeq 0.08 \text{ GeV}^2$  and  $t_+ = t_{2K} = 4m_K^2 \simeq 0.98 \text{ GeV}^2$ .

$q = q_1 + q_2$	charged kaon		neutral kaon	
	z-model	SHHKS '22	z-model	SHHKS '22
- 1.0	0.000043	0.000070	0.000024	0.000025
0.0	0.00019	0.00031	0.000084	0.000089
1.0	0.0010	0.0015	0.00033	0.00035
2.0	0.0079	0.010	0.0014	0.0015
3.5	0.63	0.65	0.015	0.015

TABLE I. Values of the quantity  $4m_K^2 \chi_{\text{extra}}[f]$ , given by Eq. (20) with  $\alpha_{th}/\pi = 0.1823$ , evaluated using the kinematical function  $\phi^{q_1 q_2}(z)$  with  $\phi_+(z_+) = (1536\pi)^{-1/2} (1 + z_+)^2 \sqrt{1 - z_+}$  and adopting for the form factor either the dispersive results of Ref. [37], labelled as SHHKS '22, or the resonance model given by Eqs. (57)-(58), labelled as z-model.

kaon channel the resonance model underestimates the contribution  $\chi_{\text{extra}}[f]$  up to  $\simeq 30 - 40\%$  for  $q \lesssim 1$ .

The values obtained for  $4m_K^2 \chi_{\text{extra}}[f]$  can be compared with the contribution  $4m_K^2 \chi_+[f]$  related to the pair-production arc. Using the resonance model we get  $4m_K^2 \chi_+[f] = 0.0024$  and  $0.0020$  for the charged and neutral channel, respectively. Using the dispersive form factor of Ref. [37] (known up to  $t \simeq 1.2 \text{ GeV}^2$  with the addition of a pQCD tail for  $t > 1.2 \text{ GeV}^2$ ) we obtain similar results, namely  $4m_K^2 \chi_+[f] = 0.0026$  and  $0.0025$  for the charged and neutral channels<sup>11</sup>. As expected from the comparison made in the right panel of Fig. 4, the contribution

<sup>11</sup> If one limits the calculation of  $4m_K^2 \chi_+[f]$  to the kinematical region of the  $\phi(1020)$  resonance, i.e. between

$\chi_{\text{extra}}[f]$  strongly depends on the value of  $q$ ; in particular, at  $q = 7/2$  it is  $\simeq 2000$  times the one at  $q = 0$ . Moreover, while at  $q = 0$  the value of  $\chi_{\text{extra}}[f]$  is only a fraction of the pair-production contribution  $\chi_+[f]$ , at  $q = 7/2$  it becomes much larger by a factor  $\simeq 240$ . The impact of the above numerical values in the implementation of the double dispersive bound in the case of the electromagnetic kaon form factor will be presented in the next Section.

Before closing this Section, we stress that presently we are not aware of a strategy to calculate a dispersive bound  $\chi_{\text{extra}}^U$ , based on first-principles only, without requiring the knowledge of the form factor outside the pair-production arc. Once this problem will be solved in terms of suitable Euclidean correlation functions calculable on the lattice, it is likely that also the choice of the kinematical function  $\phi(z)$  outside the pair-production arc will become unique.

## VI. ANALYSIS OF THE SPACELIKE EXPERIMENTAL AND LATTICE DATA ON THE CHARGED KAON FORM FACTOR

In this Section we apply the BGL  $z$ -expansion, described in Section II, to the study of the experimental data on the electromagnetic form factor of the charged kaon,  $F_{K^\pm}^{(em)}(Q^2)$ , available for spacelike values of  $Q^2 \equiv -t$  up to  $Q^2 \simeq 0.12 \text{ GeV}^2$  from FNAL [6] and CERN NA7 [7]. Separately, we consider also the recent lattice QCD results, obtained by the HotQCD Collaboration [8] using  $N_f = 2 + 1$  flavors of highly improved staggered quarks. Their results exhibit a remarkable high precision and cover a quite extended range of  $Q^2$  up to  $Q^2 \simeq 28 \text{ GeV}^2$ .

We want to compare the results obtained using the truncated BGL expansion (31) applying either the double bound represented by Eqs. (32)-(33) or the single, total bound (34). In addition we apply also the expansion (37) with the unitarity constraint (38), as described in Section II D. We remind that such an expansion, adopted in Refs. [22, 23], is equivalent to an expansion of the form factor in terms of Szegő polynomials, proposed in Refs. [19–21], but it implements the unitarity constraint in an incomplete way, i.e., only on the pair-production arc.

For the dispersive bound corresponding to the pair-production arc,  $\chi_+^U$ , we use the estimate

$$\chi_+^U = 0.0024 \pm 0.0005, \quad (68)$$

obtained using the resonance model of Section IV and assuming a 20% uncertainty. As for the contribution outside the pair-production arc,  $\chi_{\text{extra}}^U$ , this depends upon the choice of the kinematical function  $\phi^{q_1 q_2}(z)$ , defined in Eq. (65). In what follows we compare two choices: the first one is  $q_1 = q_2 = 0$  and the other one is  $q_1 = 5$  and  $q_2 = -3/2$ , which correspond respectively to  $q = q_1 + q_2$  equal to  $q = 0$  and  $q = 3.5$ . These two choices correspond to quite different values of  $\chi_{\text{extra}}^U$ , shown in Table I. Here below, we adopt the values corresponding to the dispersive form factor of Ref. [37] (known up to  $t \simeq 1.2 \text{ GeV}^2$  with the addition of a pQCD tail for  $t > 1.2 \text{ GeV}^2$ ), namely

$$\chi_{\text{extra}}^U = 0.00031 \pm 0.00006 \quad \text{for } q = 0, \quad (69)$$

$$\chi_{\text{extra}}^U = 0.65 \pm 0.13 \quad \text{for } q = 3.5, \quad (70)$$

where we have assumed again a 20% uncertainty<sup>12</sup>. Indeed, in the first case  $q = 0$  the contribution  $\chi_{\text{extra}}^U$  is a fraction of the order of 10% of the pair-production bound (68), while in the second case  $q = 3.5$ , it is much larger than  $\chi_+^U$  by a factor of  $\approx 240$ .

---

<sup>12</sup>  $t_{2K} \simeq 0.98 \text{ GeV}^2$  and  $1.2 \text{ GeV}^2$ , one gets  $4m_K^2 \chi_+[f] = 0.0024$  for both charged and neutral channels. In this way the quantities  $\chi_+^U$  and  $\chi_{\text{extra}}^U$  can be treated as uncorrelated.

In the case of the experimental data on  $F_{K^\pm}^{(em)}(Q^2)$  there are 10 data from FNAL [6] and 15 data from CERN [7]. To ensure charge conservation we add a further data point  $F_{K^\pm}^{(em)}(Q^2 = 0) = 1$  with a tiny error ( $\simeq 10^{-12}$ )<sup>13</sup>. Therefore, we have a total of  $N_{data} = 26$  data points. The covariance matrices of the two experiments are known separately, so that we can construct the full covariance matrix  $C_{ij}$  of the input data by considering the two experiments uncorrelated.

In the case of the LQCD results of the HotQCD Collaboration [8] there are 28 data points available up to  $Q^2 \simeq 28 \text{ GeV}^2$ . In our analysis we include only the first 7 points up to  $Q^2 \simeq 0.4 \text{ GeV}^2$  and compare our extrapolation at larger  $Q^2$  with the lattice points. Adding the normalization point  $F_{K^\pm}^{(em)}(Q^2 = 0) = 1$  we have a total of  $N_{data} = 8$  data points in the analysis. The covariance matrix of the data is not provided in Ref. [8]. Therefore, we consider an uncorrelated covariance matrix  $C_{ij}$ .

Let us start with the case of the experimental data on the charged kaon form factor and the choice  $q = 0$  for the kinematical function outside the pair-production arc. We apply the truncated BGL expansion (31) at various order  $M$  of the truncation using either the double bound (32)-(33) or the single, total bound (34). The dispersive bounds  $\chi_+^U$  and  $\chi_{\text{extra}}^U$  are given by Eqs. (68)-(69) and, therefore, at  $q = 0$  the total bound  $\chi^U = \chi_+^U + \chi_{\text{extra}}^U$  is largely dominated by the pair-production bound  $\chi_+^U$ . We observe a nice stability of the extrapolated form factor up to  $Q^2 \simeq 1 \text{ GeV}^2$  for  $M \geq 6$ . We apply also the expansion (37) with the unitarity constraint (38), restricted to the pair-production arc only. A reasonable stability of the results for the form factor up to  $Q^2 \simeq 1 \text{ GeV}^2$  is observed against the order  $M$  of the truncation for  $M \geq 6$ .

The comparison of the predicted bands for the form factor up to  $Q^2 \simeq 1 \text{ GeV}^2$  is shown in Fig. 5, where we have truncated all the  $z$ -expansions at order  $M = 8$ . In what follows the width of the bands will be always provided at  $1\sigma$  level. For the three expansions the value of the reduced (correlated)  $\chi^2$ -variable turns out to be equal to  $\chi^2/(d.o.f.) \simeq 1.3$ . Few comments are in order.

- The application of the double bound (32)-(33) on the BGL expansion (31) leads to the most precise extrapolation at large  $Q^2$ . In particular, it improves by a factor of  $\sim 2$  the prediction at  $Q^2 \sim 1 \text{ GeV}^2$  with respect to the application of the single, total bound (34).
- The use of the expansion (37) with the pair-production bound (38) alone, leads to a quite huge spread of values at large  $Q^2$ . This is related to the fact that the expansion in terms of Szegő polynomials, proposed in Refs. [19–21] and adopted also in Refs. [22, 23], represents an incomplete application of the unitarity constraints and it may produce violations of the unitarity constraint outside the pair-production arc and, consequently, of the total bound  $\chi^U$  on the full arc. Indeed, in the case at hand we observe that the coefficients  $b_k$  of the expansion (37) have large numerical values, leading to  $\sum_{k=0}^M b_k^2 \gg \chi^U/\chi_+^U \simeq 1.1$ .
- All the three  $z$ -expansions are consistent with the more precise dispersive results from Ref. [37] both at low and large values of  $Q^2$ . Such a high-precision level is related to the fact that the results of Ref. [37] are obtained from a global dispersive analysis of both spacelike and timelike data by implementing Eq. (56) in the isovector channel, using data on the pion electromagnetic form factor and the  $\pi\pi \rightarrow \bar{K}K$  partial-wave amplitude, and by considering in the isoscalar channel the contributions from  $\omega$ - and  $\phi$ -meson residues, determined from electromagnetic reactions involving kaons.

We have performed an analogous analysis by replacing the experimental data with the LQCD results of the HotQCD Collaboration [8]. These are much more precise than the experimental

---

<sup>13</sup> Choosing  $t_0 = t_- = 0$  in Eq. (11), this is equivalent to fix the coefficients  $a_0$  of the BGL expansion (31) to the value  $a_0 = \phi(z = 0)/\sqrt{\chi^U}$ .

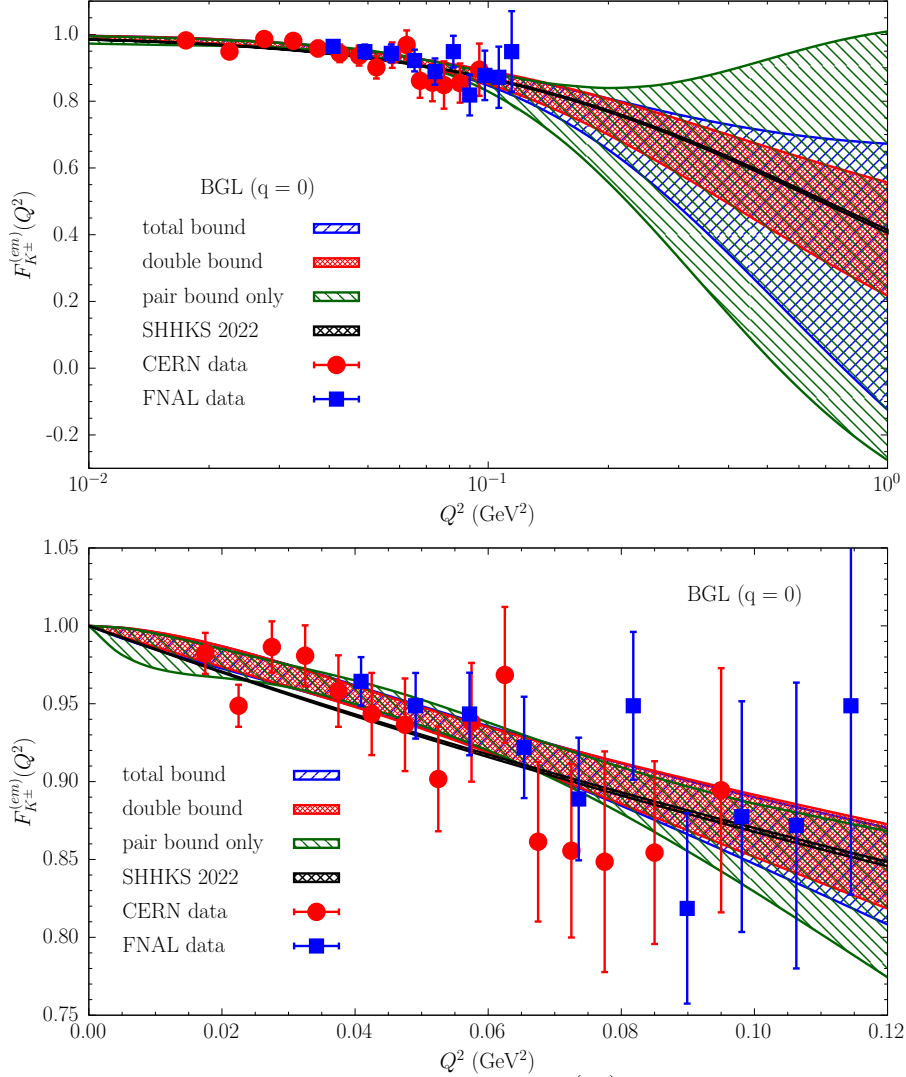


FIG. 5. The electromagnetic form factor of the charged kaon  $F_{K^\pm}^{(em)}(Q^2)$  versus the 4-momentum transfer  $Q^2 = -t$ . The red and blue bands, evaluated at  $1\sigma$  level, correspond to the results obtained using the BGL expansion (31) at  $M = 8$  and adopting respectively the double bound (32)-(33) and the single, total bound (34). The dispersive bounds  $\chi_+^U$  and  $\chi_{\text{extra}}^U$  are given respectively by Eqs. (68) and (69), and the total bound  $\chi^U$  is  $\chi^U = \chi_+^U + \chi_{\text{extra}}^U$ . The green band represents the results obtained using the expansion (37) with the unitarity constraint (38) corresponding to the pair-production arc only. In all cases the choice  $q = 0$  for the kinematical function  $\phi^{q_1 q_2}(z)$  is considered. The black band (having tiny errors) corresponds to the results of the dispersive approach of Ref. [37], while the blue squares and the red circles are respectively the experimental data from the FNAL [6] and CERN [7] experiments. The bottom panel is a zoom in the range of values of  $Q^2$  covered by the two experiments.

determinations of  $F_{K^\pm}^{(em)}(Q^2)$  by approximately one order of magnitude. As already anticipated, we include in the analysis only the lattice points up to  $Q^2 \simeq 0.4 \text{ GeV}^2$  and extrapolate our  $z$ -expansions up to  $Q^2 \simeq 28 \text{ GeV}^2$  to compare with the remaining LQCD data. The results are collected in Fig. 6, where the  $z$ -expansions are truncated at order  $M = 6$ . We observe again

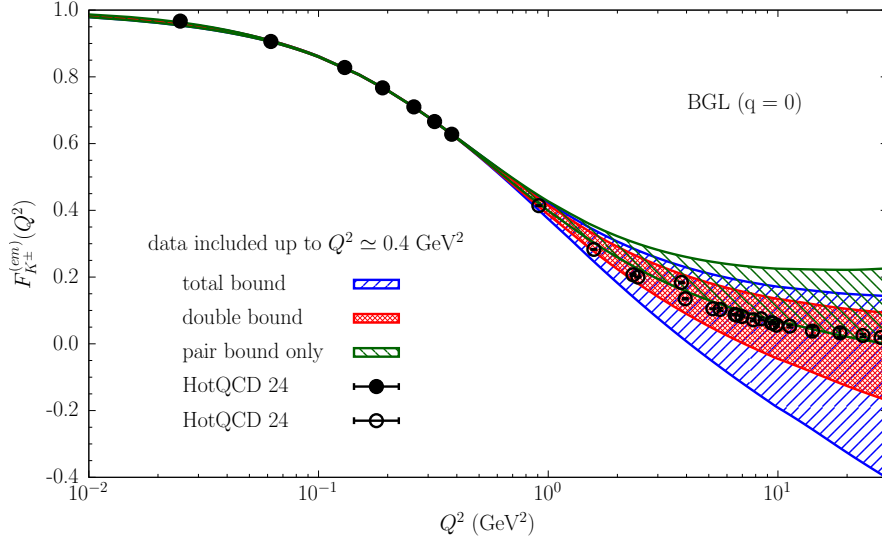


FIG. 6. The same as in the upper panel of Fig. 5, but adopting the LQCD results of the HotQCD Collaboration [8]. The data included in the analysis are those with  $Q^2 \lesssim 0.4 \text{ GeV}^2$  (full circles), while the ones not included in the analysis and extending up to  $Q^2 \simeq 28 \text{ GeV}^2$  are represented by the empty circles. All  $z$ -expansions are truncated at order  $M = 6$ .

that: i) the use of the double bound improves the extrapolation at large  $Q^2$  by a factor of  $\sim 2$  with respect to the use of the single, total bound; ii) the two BGL expansions implementing properly the unitarity constraints are nicely consistent with the lattice QCD data up to  $Q^2 \simeq 28 \text{ GeV}^2$ , and iii) the expansion in terms of Szegő polynomials, which takes into account only the unitarity constraint on the pair-production arc, is only marginally consistent with the lattice QCD data at large  $Q^2$ .

We now move to the other choice considered for the kinematical function  $\phi^{q_1 q_2}(z)$ , namely  $q = q_1 + q_2 = 3.5$ . For the bound  $\chi_{\text{extra}}^U$  we use the estimate given by Eq. (70), which is much larger than the pair-production contribution  $\chi_+^U$ , given by Eq. (68), by a factor of  $\approx 240$ . Thus, at  $q = 3.5$  the total bound  $\chi^U = \chi_+^U + \chi_{\text{extra}}^U$  is largely dominated by the contribution  $\chi_{\text{extra}}^U$  outside the pair-production arc. In what follows we will limit ourselves to the two BGL expansions properly compatible with unitarity constraints, i.e. those based on Eq. (31) with either the double bound (32)-(33) or the single, total bound (34).

The comparison of the predicted bands for  $F_{K^\pm}^{(em)}(Q^2)$ , obtained using simultaneously the two experimental datasets from FNAL [6] and CERN [7], is shown in Fig. 7, where we have truncated the  $z$ -expansions at order  $M = 8$ . For the two expansions the value of the reduced (correlated)  $\chi^2$ -variable turns out to be equal to  $\chi^2/(d.o.f.) \simeq 1.4$ . It is confirmed that also in the case  $q = 3.5$  the use of the double bound yields a much more precise band of values at large  $Q^2$  with respect to the use of the single total bound. By comparing the results in Figs. 5 and 7 there is a clear dependence of the extrapolated band on the choice of  $q$  in the case of the single total bound, while such a dependence is much more limited in the case of the double bound.

Adopting the LQCD results from the HotQCD Collaboration [8] the results obtained with our BGL expansions, truncated at order  $M = 6$ , are collected in Fig. 8. Both BGL expansions, including only lattice points with  $Q^2 \lesssim 0.4 \text{ GeV}^2$ , predict values consistent with the lattice QCD data up to  $Q^2 \simeq 28 \text{ GeV}^2$  though within a much larger band of values with respect to the choice  $q = 0$  (compare with Fig. 6). Moreover, an anomalous increase of the width of the predicted bands is visible also at low  $Q^2$ , i.e. in the  $Q^2$ -range of values adopted in the fitting procedure.

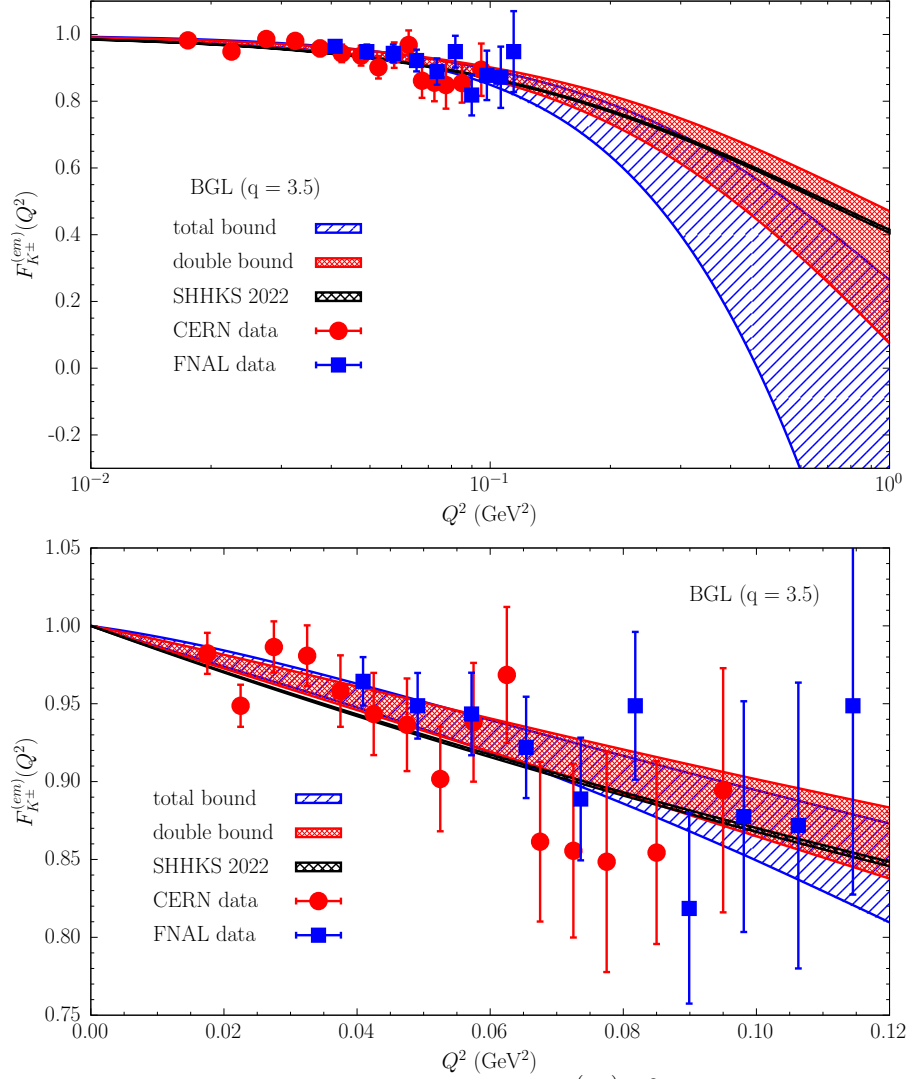


FIG. 7. The electromagnetic form factor of the charged kaon  $F_{K^\pm}^{(em)}(Q^2)$  versus the 4-momentum transfer  $Q^2 = -t$ . The red and blue bands, evaluated at  $1\sigma$  level, correspond to the results obtained using the BGL expansion (31) at  $M = 8$  and adopting respectively the double bound (32)-(33) and the single, total bound (34). The dispersive bounds  $\chi_+^U$  and  $\chi_{\text{extra}}^U$  are given respectively by Eqs. (68) and (70), and the total bound  $\chi^U$  is  $\chi^U = \chi_+^U + \chi_{\text{extra}}^U$ . In all cases the choice  $q = 3.5$  for the kinematical function  $\phi^{q_1 q_2}(z)$  is considered. The black band, blue squares and red circles are as in Fig. 5. The bottom panel is a zoom in the range of values of  $Q^2$  covered by the two experiments.

Both unpleasant features are related to the presence of non-unitary effects in the set of input data. The removal of such effects is discussed in the next subsection.



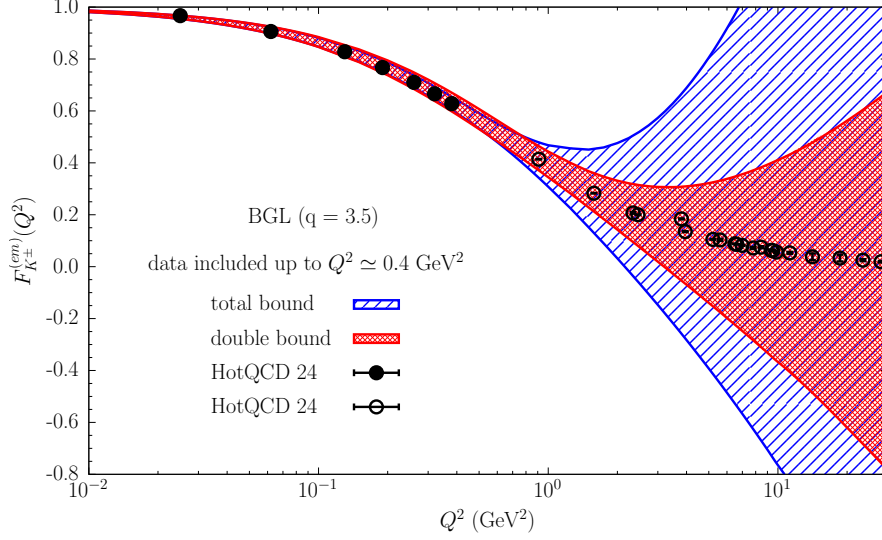


FIG. 8. The same as in the upper panel of Fig. 7, but adopting the LQCD results of the HotQCD Collaboration [8]. The data included in the analysis are those with  $Q^2 \lesssim 0.4 \text{ GeV}^2$  (full circles), while the ones not included in the analysis and extending up to  $Q^2 \simeq 28 \text{ GeV}^2$  are represented by the empty circles. All  $z$ -expansions are truncated at order  $M = 6$ .

#### A. Unitary filtering of the input data

According to Ref. [1], in order to have a completely unitary BGL approach any given set of input data  $\{f_i \equiv F_{K^\pm}^{(em)}(Q_i^2)\}$  (with  $i = 1, 2, \dots, N_{data}$ ) should be filtered against the single total bound  $\chi^U$ ; more precisely, the following constraint should be fulfilled

$$\chi[\beta] \leq \chi^U = \chi_{\text{extra}}^U + \chi_+^U, \quad (71)$$

where the function  $\beta(z)$  is given by

$$\beta(z) = \frac{1}{\phi(z)B(z)d(z)} \sum_{i=1}^{N_{data}} \phi(z_i)B(z_i)d_i f_i \frac{1-z_i^2}{z-z_i} \quad (72)$$

and

$$\begin{aligned} \chi[\beta] &\equiv \frac{1}{2\pi i} \oint_{|z|=1} \frac{dz}{z} |\phi(z)\beta(z)|^2 \\ &= \sum_{i,j=1}^{N_{data}} \phi(z_i)B(z_i)d_i f_i \phi(z_j)B(z_j)d_j f_j \frac{(1-z_i^2)(1-z_j^2)}{1-z_i z_j} \end{aligned} \quad (73)$$

with

$$\begin{aligned} d(z) &= \prod_{m=1}^{N_{data}} \frac{1-z z_m}{z-z_m}, \\ d_i &= \prod_{m \neq i=1}^{N_{data}} \frac{1-z_i z_m}{z_i-z_m}, \end{aligned}$$

Starting from the original covariance matrix  $C_{ij}$  for the input data, the action of the filter (71) is to select the unitary subset  $\{\bar{f}_i\}$  with a covariance matrix  $\bar{C}_{ij}$ , i.e. only those data that can be reproduced exactly by (an infinite number of) unitary BGL expansions, given by Eq. (12) with the constraint (16). When the filter (71) is not fulfilled, then the input data cannot be reproduced exactly by any unitary BGL expansion. These data contain non-unitary effects and they are removed from the analysis (see for details Ref. [1]). Therefore, to the subset of input data satisfying the global filter (71) we apply the expansion (31), adopting the single total bound (34) for the coefficients of the expansion.

In the case of the analysis employing the double bound (32)-(33) we modify the selection of the unitary input data as follows. Since  $\chi[\beta]$  is the integral over the unit circle given in Eq. (73), we can split such an integral into the sum of two (positive) contributions, related to the pair-production arc and outside the pair-production arc, namely

$$\chi[\beta] = \chi_{\text{extra}}[\beta] + \chi_{\text{pair}}[\beta] \quad (74)$$

where

$$\chi_{\text{pair}}[\beta] = \sum_{i,j=1}^{N_{\text{data}}} \phi(z_i) B(z_i) d_i f_i \phi(z_j) B(z_j) d_j f_j \frac{(1-z_i^2)(1-z_j^2)}{1-z_i z_j} [1 - B_{ij}(\alpha_{th})] , \quad (75)$$

$$\chi_{\text{pair}}[\beta] = \sum_{i,j=1}^{N_{\text{data}}} \phi(z_i) B(z_i) d_i f_i \phi(z_j) B(z_j) d_j f_j \frac{(1-z_i^2)(1-z_j^2)}{1-z_i z_j} B_{ij}(\alpha_{th}) \quad (76)$$

with

$$\begin{aligned} B_{ij}(\alpha_{th}) &\equiv \frac{1-z_i z_j}{2\pi} \int_{-\alpha_{th}}^{\alpha_{th}} d\alpha \frac{1}{1+z_i z_j - (z_i + z_j) \cos \alpha + i(z_j - z_i) \sin \alpha} , \\ &= 1 - \frac{1}{\pi} \left\{ \text{Arctg} \left[ \frac{1-z_i}{1+z_i} \cotg \left( \frac{\alpha_{th}}{2} \right) \right] + \text{Arctg} \left[ \frac{1-z_j}{1+z_j} \cotg \left( \frac{\alpha_{th}}{2} \right) \right] \right\} \end{aligned} \quad (77)$$

and  $\alpha_{th}$  given by Eq. (18). Then, we may replace the global filter (71) with the double filter

$$\chi_{\text{extra}}[\beta] \leq \chi_{\text{extra}}^U , \quad (78)$$

$$\chi_{\text{pair}}[\beta] \leq \chi_+^U . \quad (79)$$

Therefore, to the subset of input data satisfying the double filter (27)-(26) we apply the expansion (31), adopting the double bound (32)-(33) for the coefficients of the expansion.

In the kaon case of interest in this paper there are no poles below the lowest threshold  $t_{th} = 4m_\pi^2 \simeq 0.08 \text{ GeV}^2$  and, therefore,  $B(z) = 1$ . We apply either the global filter (71) or the double filter (78)-(79). The main effect of such filters is a modification of the original covariance matrix  $C_{ij}$  into a new matrix  $\bar{C}_{ij}$  by introducing appropriate correlations either between the two experimental datasets or among the LQCD data. We stress that such modifications are dictated by unitarity. It turns out that in the case of the experimental data from FNAL [6] and CERN [7] the impact of the filtering procedure described above on the predicted bands of values for the form factor is limited, while this is not the case when the LQCD data from the HotQCD Collaboration [8] are considered. This is likely due to the facts that correlations are not provided in Ref. [8] and the LQCD points exhibit a remarkable high precision (at the level of few permille). Consequently, the global filter (71) or the double filter (78)-(79) produce a new highly correlated covariance matrix  $\bar{C}_{ij}$ . The new predicted bands for the form factor  $F_{K^\pm}^{(em)}(Q^2)$  are shown in Fig. 9 and the impact of the filtering procedures is clearly visible by a direct comparison with

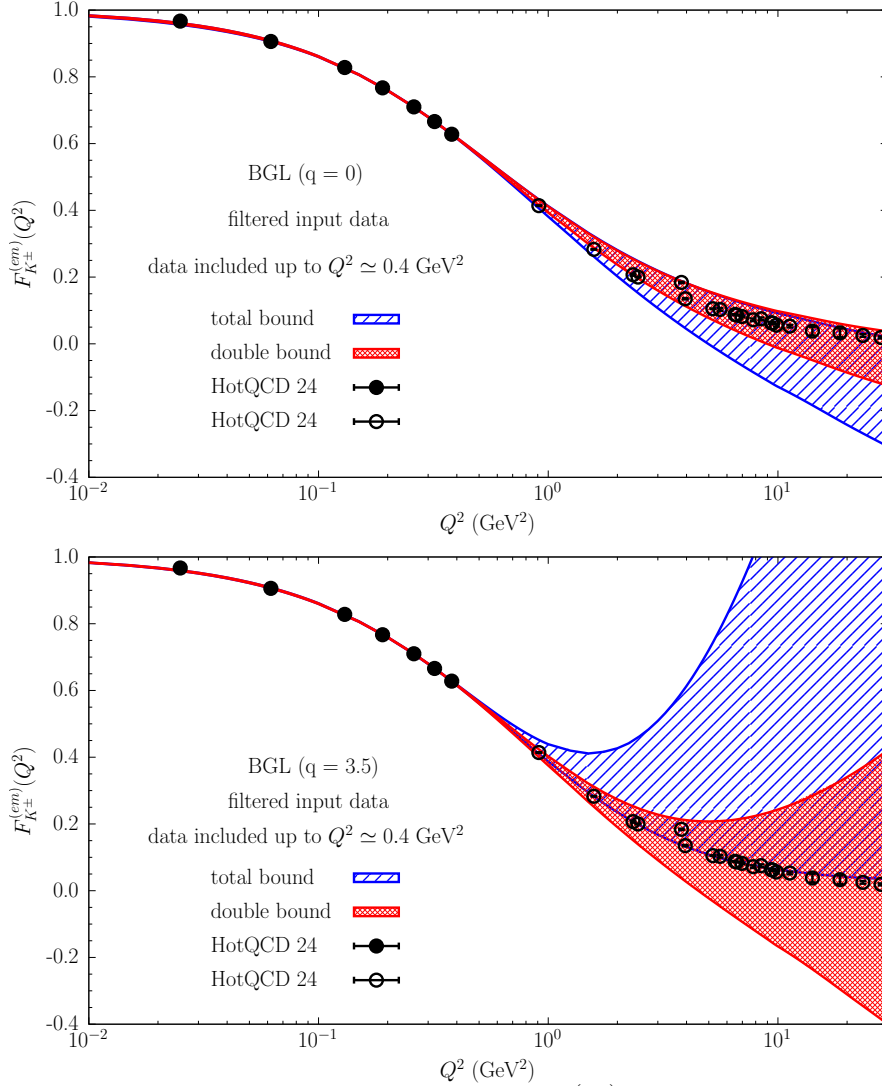


FIG. 9. The electromagnetic form factor of the charged kaon  $F_{K^\pm}^{(em)}(Q^2)$  versus the 4-momentum transfer  $Q^2 = -t$ , adopting the LQCD results of the HotQCD Collaboration [8]. The data included in the analysis are those with  $Q^2 \lesssim 0.4 \text{ GeV}^2$  (full circles), while the ones not included in the analysis and extending up to  $Q^2 \simeq 28 \text{ GeV}^2$  are represented by the empty circles. The upper panel refers to the choice  $q = 0$  for the kinematical function  $\phi^{q_1 q_2}(z)$ , while the lower panel to the choice  $q = 3.5$ . The red and blue bands, evaluated at  $1\sigma$  level, correspond to the results obtained using the BGL expansion (31) at  $M = 6$  and adopting respectively the double bound (32)-(33) and the single, total bound (34). The dispersive bounds  $\chi_+^U$  and  $\chi_{\text{extra}}^U$  are described in the text (see Eqs. (68)-(70)) and the total bound  $\chi^U$  is  $\chi^U = \chi_+^U + \chi_{\text{extra}}^U$ . The input data are filtered either by the global filter (71) or by the double filter (78)-(79), according to the unitarity constraints applied to the coefficients of the BGL expansions.

Figs. 6 and 8. The anomalous increase of the width of the predicted bands at low  $Q^2$ , visible in Fig. 8, is completely eliminated. Moreover, at large  $Q^2$  the width of the predicted bands is reduced significantly both at  $q = 0$  and  $q = 3.5$ . Note that the predictions of the double bound expansion are nicely consistent with the LQCD points up to  $Q^2 \simeq 28 \text{ GeV}^2$  both at  $q = 0$  and

$q = 3.5$ , while those corresponding to the total bound expansion are only marginally consistent. Finally, the most precise predictions at large  $Q^2$  are those corresponding to the double bound expansion with the choice  $q = 0$ .

### B. Charged kaon radius

A quantity of phenomenological interest is the charged kaon radius  $r_{K^\pm}$ , defined through the relation

$$r_{K^\pm}^2 = -6 \frac{dF_{K^\pm}^{(em)}(Q^2)}{dQ^2} \Big|_{Q^2=0} . \quad (80)$$

In the experimental works from FNAL [6] and CERN [7] the charged kaon radius is estimated from the data assuming a simple Ansatz of the form  $F_{K^\pm}^{(em)}(Q^2) = 1/(1 + r_{K^\pm}^2 Q^2/6)$ , obtaining  $r_{K^\pm} = 0.53 \pm 0.05$  fm [6] and  $r_{K^\pm} = 0.58 \pm 0.04$  fm [7]. These two determinations are averaged in the last PDG review [9], leading to  $r_{K^\pm} = 0.560 \pm 0.031$  fm.

We point out, however, that the monopole Ansatz used in Refs. [6, 7] represents a model-dependent assumption, which might lead to an underestimation of the uncertainty. Using the same experimental datasets, but adopting the results of our model-independent BGL  $z$ -expansions with unitarity implemented through the double dispersive bounds we get

$$r_{K^\pm} = 0.538 \pm 0.066 \pm 0.004_q [0.066] \quad [\text{FNAL} + \text{CERN data}] , \quad (81)$$

where the second error comes from the small dependence upon the choice of the kinematical function (estimated using our results obtained at  $q = 0$  and  $q = 3.5$ ). Thus, the value quoted by PDG underestimates the uncertainty by a factor of  $\simeq 2$  due to the model-dependent assumption about the momentum dependence of the charged kaon form factor.

In the case of LQCD data the authors of Ref. [8] provide the quite precise estimate  $r_{K^\pm} = 0.600 \pm 0.002$  fm, based on fitting their data up to  $Q^2 \simeq 0.4$  GeV<sup>2</sup> adopting a vector-meson-dominance Ansatz constructed using the three main resonances  $\rho(770)$ ,  $\omega(780)$  and  $\phi(1020)$  with masses taken from the PDG [9]. Using the same LQCD dataset, but adopting the results of our *model-independent* BGL  $z$ -expansions with unitarity implemented through the double dispersive bounds we get

$$r_{K^\pm} = 0.641 \pm 0.022 \pm 0.001_q [0.022] \quad [\text{LQCD data}] , \quad (82)$$

which is consistent within  $\simeq 2\sigma$  with the estimate made in Ref. [8], but with an uncertainty ten times larger. Note that, thanks to the use of the double dispersive bound, the dependence of our result (82) upon the choice of the kinematical function (i.e., the choice of  $q$ ) is almost negligible.

## VII. CONCLUSIONS

We have discussed a specific application of the framework of multiple dispersive bounds, firstly introduced in the companion paper [1], to the study of sub-threshold branch-cuts. The main results are as follows.

- In the standard BGL  $z$ -expansion we have proposed a double dispersive bound as the proper way to deal with the presence of sub-threshold branch-cuts in accordance with unitarity. The key idea is that two different unitarity constraints have to be considered at the same time, namely the first one in the pair-production arc and the second one in the extra

region between the lowest sub-threshold and the pair-production branch-points. We have highlighted that the bound related to the extra region,  $\chi_{\text{extra}}^U$ , is not related to the usual susceptibilities, i.e. to the quantities coming from the computation of the derivatives of appropriate two-point Green functions in momentum space. It remains an open issue to understand the proper Euclidean correlation functions that would give direct access to the bound  $\chi_{\text{extra}}^U$  directly from first-principles, e.g. from lattice simulations.

- We have developed a simple resonance model in order to take into account the effects of above-threshold poles on the description of hadronic form factors. We have successfully checked our model against the effects of the  $\rho(770)$ -meson resonance on the electromagnetic form factor of the pion. Then, we have extended our model to the case of the electromagnetic form factors of the charged and neutral kaons and we have successfully compared it with the dispersive results of Ref. [37].
- We have pointed out that the choice of the outer function outside the pair-production arc is not unique. Possible choices have been discussed and used to evaluate the dispersive bound  $\chi_{\text{extra}}^U$ .
- We have analyzed the experimental data or the lattice QCD (LQCD) results available for the electromagnetic form factor of the charged kaon in the spacelike-region. The comparison with other methodologies present in literature and with the BGL  $z$ -expansion based on the single, total dispersive bound has clearly shown that the  $z$ -expansion including the double dispersive bound provides the most precise extrapolation at large momentum transfer as well as the most stable results with respect to the choice of the outer function outside the pair-production region.
- We have highlighted the impact of the application of the unitarity filter on the given set of input data (see Section VI A and Ref. [1]) and we have compared our model-independent findings for the charged kaon radius with the model-dependent estimates made in the last PDG review [9] and in Ref. [8] (see Section VI B).

We leave the investigation of multiple dispersive bounds to other physical processes of interest, such as weak semileptonic decays of hadrons, to future dedicated works.

## ACKNOWLEDGEMENTS

We warmly thank Guido Martinelli for all the insightful discussions we had together and for his continuous support. We are deeply indebted with the authors of Ref. [37] for having provided us with the numerical results of their dispersive analysis for the charged kaon form factor  $F_{K^\pm}^{(em)}(t)$  both in the spacelike sector down to  $t \simeq -1 \text{ GeV}^2$  and in the timelike one up to  $t \simeq 1.2 \text{ GeV}^2$ . S.S. is supported by the Italian Ministry of University and Research (MUR) under grant PRIN 2022N4W8WR. L.V. is supported by the Italian Ministry of University and Research (MUR) and by the European Union's NextGenerationEU program under the Young Researchers 2024 SoE Action, research project 'SHYNE', ID: SOE\_20240000025.

## Appendix A: Riemann sheets in terms of the conformal variable

For a complex number  $x + iy = re^{i\theta}$ , where  $r = \sqrt{x^2 + y^2}$  and  $-\pi < \theta \leq \pi$ , the common choice is that in the first Riemann sheet (labelled as  $I$ ) the real part of  $\sqrt{x + iy}$  is nonnegative,

namely

$$\left[\sqrt{x+iy}\right]^I = \sqrt{r}e^{i\theta/2} = \sqrt{\frac{r+x}{2}} + i\operatorname{sgn}(y)\sqrt{\frac{r-x}{2}}, \quad (\text{A1})$$

while in the second Riemann sheet (labelled as  $II$ ) one has

$$\left[\sqrt{x+iy}\right]^{II} = \sqrt{r}e^{i(\theta+2\pi)/2} = -\sqrt{r}e^{i\theta/2} = -\sqrt{\frac{r+x}{2}} - i\operatorname{sgn}(y)\sqrt{\frac{r-x}{2}}. \quad (\text{A2})$$

This implies that  $[\sqrt{t_+-t}]^I = -[\sqrt{t_+-t}]^{II}$ , so that  $[z_+]^I = 1/[z_+]^{II}$ . With the above choice of the principal value of the square root the first Riemann sheet corresponds to values of the conformal variable  $z_+$  always inside the unit disk (i.e.,  $|z_+| < 1$ ), while in the second Riemann sheet the values of  $z_+$  lie always outside the unit disk (i.e.,  $|z_+| > 1$ ). On the branch-cut one has  $[[z_+]]^I = [[z_+]]^{II} = 1$ .

### Appendix B: Truncation errors in the BGL expansion

Following Ref. [5], the absolute difference between the true representation

$$\frac{\phi(z)B(z)f(z)}{\sqrt{\chi^U}} = \sum_{k=0}^{\infty} a_k z^k \quad (\text{B1})$$

and its truncated expansion at order  $M$

$$\frac{\phi(z)B(z)f^{(M)}(z)}{\sqrt{\chi^U}} = \sum_{k=0}^M a_k z^k \quad (\text{B2})$$

has an upper limit for real values of  $z$  given by

$$\frac{|\phi(z)B(z)|}{\sqrt{\chi^U}} |f(z) - f^{(M)}(z)| = \left| \sum_{k=M+1}^{\infty} a_k z^k \right| \leq \sqrt{\sum_{k=M+1}^{\infty} a_k^2} \sqrt{\sum_{k=M+1}^{\infty} |z|^{2k}},$$

which, thanks to the unitarity constraint (16), implies

$$|f(z) - f^{(M)}(z)| \leq \frac{\sqrt{\chi^U}}{|\phi(z)B(z)|} \frac{|z|^{M+1}}{\sqrt{1-|z|^2}} \sqrt{1 - \sum_{k=0}^M a_k^2}. \quad (\text{B3})$$

Therefore, it may be argued [5] that, since  $|z| < 1$  (and for  $z$  far from the zeros of the Blaschke product), the truncation error (B3) monotonically decreases as  $M$  increases.

However, in practice the coefficients  $a_k$  in Eq. (B2) are typically obtained through a fitting procedure applied to a given set of input data  $\{f_i\}$ . Thus, generally speaking, at fixed  $k$  the coefficients  $a_k$  in Eq. (B2) depend on the truncation order  $M$  and, therefore, they may not coincide with the corresponding coefficients of the true representation (B1). A further contribution, related to the differences  $a_k - a_k^{(M)}$  for  $k \leq M$ , should be added to Eq. (B3), obtaining the final estimate

$$\begin{aligned} |f(z) - f^{(M)}(z)| &\leq \frac{\sqrt{\chi^U}}{|\phi(z)B(z)|} \frac{1}{\sqrt{1-|z|^2}} \left\{ |z|^{M+1} \sqrt{1 - \sum_{k=0}^M a_k^2} \right. \\ &\quad \left. + \sqrt{1-|z|^{2(M+1)}} \sqrt{\sum_{k=0}^M [a_k - a_k^{(M)}]^2} \right\}. \end{aligned} \quad (\text{B4})$$

The size of the truncation error (B4) depends also on the convergence of all the coefficients  $a_k^{(M)}$  with  $k \leq M$ . Thus, it is not guaranteed *a priori* that for a given value  $|z| < 1$  the truncation error (B4) decreases monotonically as  $M$  increases.

### Appendix C: Orthonormal polynomials

Let us consider a generic truncated  $z$ -expansion expressed in terms of the monomials  $z^k$ , viz.

$$\eta(z) = \sum_{k=0}^N b_k z^k \quad (\text{C1})$$

with  $b_k$  being (real) coefficients satisfying the off-diagonal constraint

$$\sum_{k,m=0}^N b_k U_{km} b_m \leq 1, \quad (\text{C2})$$

where the matrix  $U$  is by definition real, symmetric and positive-definite. According to the Cholesky decomposition, the matrix  $U$  can be uniquely written as  $U = LL^T$ , where  $L$  is a lower triangular matrix and  $L^T$  its transpose (an upper triangular matrix). Thus, the l.h.s. of Eq. (C2) can be rewritten in a diagonal form

$$\sum_{k,m=0}^N b_k U_{km} b_m = b^T U b = c^T c = \sum_{n=0}^N c_n^2, \quad (\text{C3})$$

where  $c = L^T b$ . Since  $U$  is positive-definite, the matrix  $L$  can be inverted and its inverse  $L^{-1}$  is still a lower triangular matrix. One gets  $b = (L^T)^{-1} c = (L^{-1})^T c$ , so that Eq. (C1) can be rewritten as

$$\eta(z) = \sum_{k=0}^N c_k p_k(z), \quad (\text{C4})$$

where

$$p_k(z) = \sum_{m=0}^N L_{km}^{-1} z^m. \quad (\text{C5})$$

Since  $L^{-1}$  is a lower triangular matrix, i.e.  $L_{km}^{-1} = 0$  for  $m > k$  and  $L_{km}^{-1} \neq 0$  for  $m \leq k$ , the polynomial  $p_k(z)$  has a degree equal to  $k$ . Note that the construction of the polynomial  $p_k(z)$  does not depend upon the polynomials with a higher degree.

In the case of the matrix  $U(\alpha_{th})$  given by Eq. (30) the corresponding polynomials (C5) are known as the (normalized) Szegő polynomials  $p_k(z; \alpha_{th})$  [24]. They are orthonormal on the arc  $-\alpha_{th} \leq \alpha \leq \alpha_{th}$ , i.e. on the unit circle  $|z| = 1$  with respect to a weight function given by  $\Theta(\alpha_{th} - |\alpha|)$ , namely

$$\begin{aligned} & \frac{1}{2\pi} \int_{-\pi}^{\pi} d\alpha \Theta(\alpha_{th} - |\alpha|) p_k(e^{i\alpha}; \alpha_{th}) p_{k'}^*(e^{i\alpha}; \alpha_{th}) \\ &= \frac{1}{2\pi} \int_{-\alpha_{th}}^{\alpha_{th}} d\alpha p_k(e^{i\alpha}; \alpha_{th}) p_{k'}^*(e^{i\alpha}; \alpha_{th}) \\ &= L_{km}^{-1} U_{mm'}(\alpha_{th}) (L^{-1})_{m'k'}^T = \delta_{kk'}. \end{aligned} \quad (\text{C6})$$

### Appendix D: Eigenvalues of the matrix $U(\alpha_{th})$

The eigenvalues  $\lambda_k$  of the matrix  $U_{kk'}(\alpha_{th})$ , given by Eq. (30), are shown in Fig. 10 for various values of the matrix dimension  $N$ . It can be seen that all such (finite) matrices have eigenvalues in the range  $(0, 1)$ .

This is related to the facts that: i) the matrix  $U(\alpha_{th})$  is positive definite (i.e.  $\vec{b}^T U(\alpha_{th}) \vec{b} > 0$  for any vector  $\vec{b} \neq \vec{0}$ ), and ii) Eq. (30) implies that  $U_{kk}(\alpha_{th}) = \alpha_{th}/\pi < 1$ , so that  $\text{Tr}[U(\alpha_{th})] = N\alpha_{th}/\pi < N$ .

The eigenvalues are approximately given by a Fermi-Dirac-like distribution<sup>14</sup>. Thus, as  $N$  increases, the distribution of the eigenvalues becomes closer and closer to an Heaviside step function, namely  $\lambda_k \rightarrow 0$  for  $k/N = 0, \dots, 1 - \alpha_{th}/\pi$  and  $\lambda_k \rightarrow 1$  for  $k/N = 1 - \alpha_{th}/\pi, \dots, 1$ .

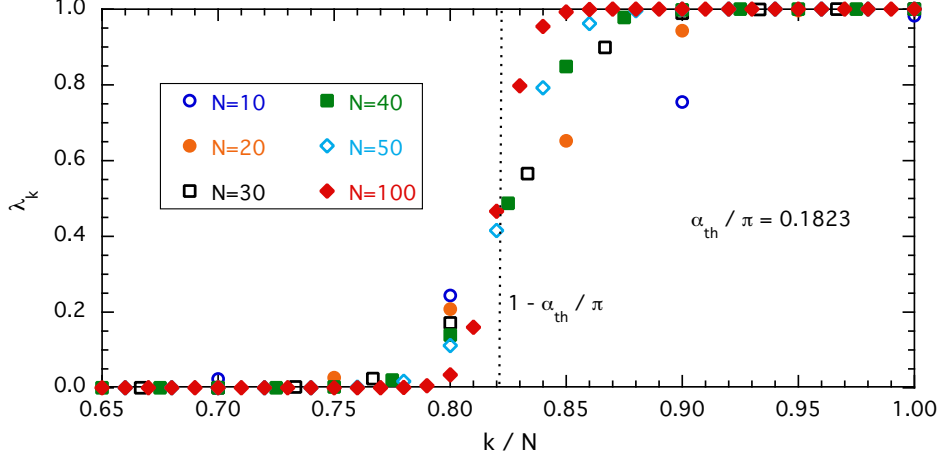


FIG. 10. Eigenvalues  $\lambda_k$  of the matrix  $U_{kk'}(\alpha_{th})$  with  $k, k' = 0, 1, \dots, N$  for various values of its dimension  $N$ . The value of the parameter  $\alpha_{th}$  is specified in the inset.

Few comments are in order.

- Since  $0 < \lambda_k < 1$ , one has

$$\sum_{k, k'=0}^N b_{k'} U_{k'k}(\alpha_{th}) b_k < \sum_{k=0}^N b_k^2. \quad (D1)$$

Thus, the diagonal constraint  $\sum_{k=0}^{\infty} a_k^2 \leq 1$ , fulfilled by the coefficients of the expansion (12), implies that the coefficients  $a_k$  satisfy also the off-diagonal constraint  $\sum_{k, k'=0}^N a_{k'} U_{k'k}(\alpha_{th}) a_k \leq 1$  related to the pair-production arc. Instead, the opposite is not guaranteed: the off-diagonal constraint  $\sum_{k, k'=0}^N b_{k'} U_{k'k}(\alpha_{th}) b_k \leq 1$  cannot guarantee that  $\sum_{k=0}^N b_k^2 \leq 1$ . This in turn implies that the truncation error (B3) of Appendix B, obtained in Refs. [4, 5], may not be applicable to the expansion (37) and, consequently, to the expansion (35).

In Fig. 11 the absolute values of few Szegő polynomials  $p_k(z; \alpha_{th})$  is shown for real values of  $z$ . It can be seen that for increasing values of  $k$  the Szegő polynomials  $p_k(z; \alpha_{th})$  are not limited inside the unit disk at variance with the monomials  $z^k$  (for which one has  $|z^k| < 1$  for  $|z| < 1$ ). This property confirms that the truncation error (B3) of Appendix B may not be applicable to the expansions (35) or (37).

- In the limit  $N \rightarrow \infty$  the eigenvalues of the matrix  $U_{kk'}(\alpha_{th})$  are either 0 or 1, i.e. the matrix  $U(\alpha_{th})$  acts as a projection. Thus, let us consider the coefficients  $b_k$  of the expansion (37) as the components of a vector  $\vec{b}$  with norm given by  $\vec{b}^T \vec{b} = \sum_{k=0}^{\infty} b_k^2$ . The vector  $\vec{b}$  can be written as the sum of two vectors

$$\vec{b} = \vec{b}^{(0)} + \vec{b}^{(1)}, \quad (D2)$$

given by ( $i = 0, 1$ )

$$\vec{b}^{(i)} = \sum_{n=0}^{\infty} c_n^{(i)} \vec{v}_n^{(i)}, \quad (D3)$$

<sup>14</sup> The eigenvalues  $\lambda_k$  can be approximated with a good accuracy by the function  $\{1 + e^{\frac{k/N - 1 + \alpha_{th}/\pi}{\sigma}}\}^{-1}$  with  $\sigma \propto 1/N$ .



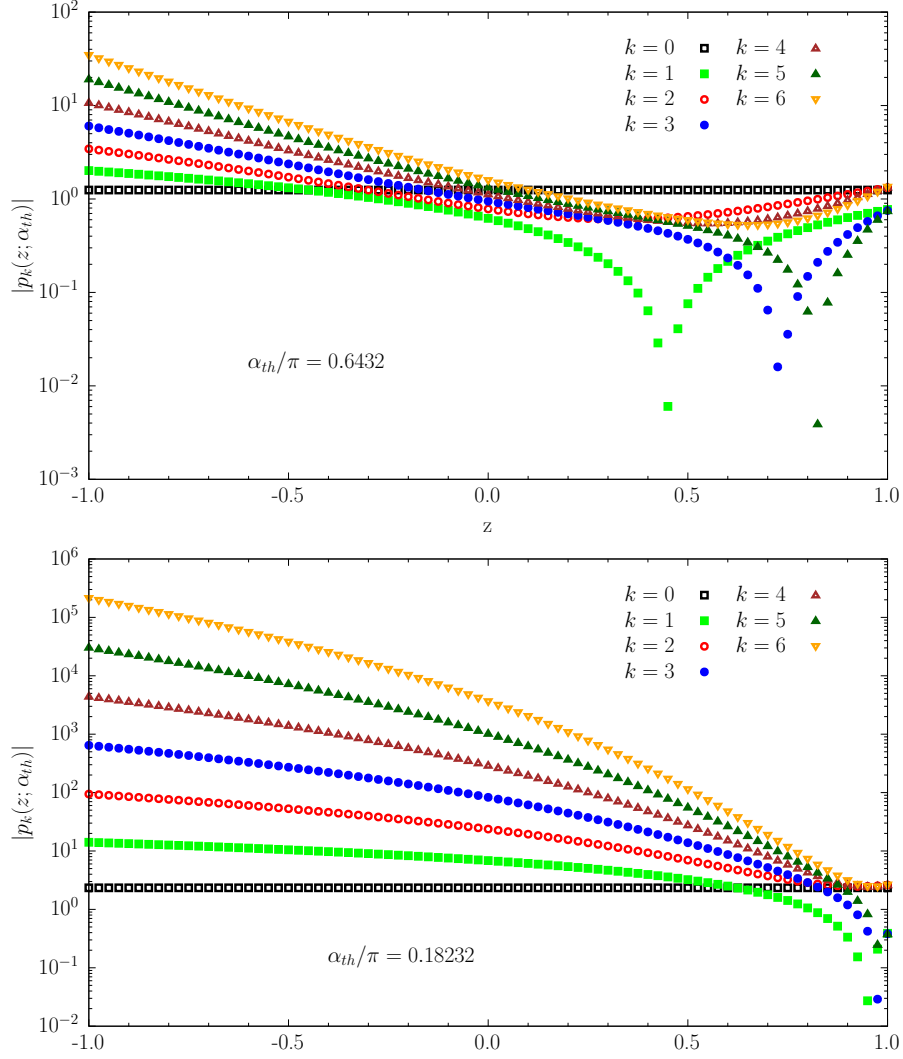


FIG. 11. The absolute values of the (normalized) Szegő polynomials  $p_k(z; \alpha_{th})$  with  $k \leq 6$  versus  $z$  for a couple of values of  $\alpha_{th}$  specified in the insets. The zero-order polynomial  $p_0(z; \alpha_{th})$  is a constant given explicitly by  $\sqrt{\pi/\alpha_{th}}$ .

where  $\vec{v}_n^{(i)}$  is the  $n$ -th eigenvector of the matrix  $U$  corresponding to eigenvalue equal to  $i$ . The off-diagonal constraint (38) is equivalent to bound only the norm of the vector  $\vec{b}^{(1)}$ , namely

$$\sum_{k,k'=0}^{\infty} b_{k'} U_{k'k}(\alpha_{th}) b_k = \sum_{k=0}^{\infty} (b_k^{(1)})^2 = \vec{b}^{(1)T} \vec{b}^{(1)} \leq 1. \quad (D4)$$

The norm of the vector  $\vec{b}^{(0)}$  as well as the norm of the full vector  $\vec{b}$  are left unbounded. Correspondingly, the  $z$ -expansion (37) can be written as the sum of two  $z$ -expansions, namely

$$f(z) = f^{(0)}(z) + f^{(1)}(z), \quad (D5)$$

where

$$f^{(i)}(z) = \frac{\sqrt{\chi_+^U}}{\phi(z)B(z)} \sum_{k=0}^{\infty} b_k^{(i)} z^k. \quad (\text{D6})$$

Only the contribution  $f^{(1)}(z)$  receives a true dispersive bound, i.e.  $\sum_{k=0}^{\infty} (b_k^{(1)})^2 \leq 1$ , while the quantity  $f^{(0)}(z)$  is unbounded.

- 
- [1] S. Simula and L. Vittorio, *Multiple dispersive bounds. I) An improved z-expansion*, .
  - [2] C.G. Boyd, B. Grinstein and R.F. Lebed, *Constraints on form-factors for exclusive semileptonic heavy to light meson decays*, *Phys. Rev. Lett.* **74** (1995) 4603 [[hep-ph/9412324](#)].
  - [3] C.G. Boyd, B. Grinstein and R.F. Lebed, *Model independent extraction of  $-V(cb)-$  using dispersion relations*, *Phys. Lett. B* **353** (1995) 306 [[hep-ph/9504235](#)].
  - [4] C.G. Boyd, B. Grinstein and R.F. Lebed, *Model independent determinations of anti-B  $\rightarrow$  D (lepton),  $D^*$  (lepton) anti-neutrino form-factors*, *Nucl. Phys. B* **461** (1996) 493 [[hep-ph/9508211](#)].
  - [5] C.G. Boyd, B. Grinstein and R.F. Lebed, *Precision corrections to dispersive bounds on form-factors*, *Phys. Rev. D* **56** (1997) 6895 [[hep-ph/9705252](#)].
  - [6] E.B. Dally et al., *DIRECT MEASUREMENT OF THE NEGATIVE KAON FORM-FACTOR*, *Phys. Rev. Lett.* **45** (1980) 232.
  - [7] S.R. Amendolia et al., *A Measurement of the Kaon Charge Radius*, *Phys. Lett. B* **178** (1986) 435.
  - [8] H.-T. Ding, X. Gao, A.D. Hanlon, S. Mukherjee, P. Petreczky, Q. Shi et al., *QCD Predictions for Meson Electromagnetic Form Factors at High Momenta: Testing Factorization in Exclusive Processes*, *Phys. Rev. Lett.* **133** (2024) 181902 [[2404.04412](#)].
  - [9] PARTICLE DATA GROUP collaboration, *Review of particle physics*, *Phys. Rev. D* **110** (2024) 030001.
  - [10] I. Caprini, *Functional Analysis and Optimization Methods in Hadron Physics*, SpringerBriefs in Physics, Springer (2019), 10.1007/978-3-030-18948-8.
  - [11] N.N. Meiman, *Analytic Expressions for Upper Limits of Coupling Constants in Quantum Field Theory*, *Sov. Phys. JETP* **17** (1963) 830.
  - [12] S. Okubo, *Exact bounds for k-l-3 decay parameters*, *Phys. Rev. D* **3** (1971) 2807.
  - [13] S. Okubo, *New improved bounds for k-l-3 parameters*, *Phys. Rev. D* **4** (1971) 725.
  - [14] S. Okubo and I.-F. Shih, *Exact inequality and test of chiral sw(3) theory in k-l-3 decay problem*, *Phys. Rev. D* **4** (1971) 2020.
  - [15] C. Bourrely, B. Machet and E. de Rafael, *Semileptonic Decays of Pseudoscalar Particles ( $M \rightarrow M' \ell \nu_\ell$ ) and Short Distance Behavior of Quantum Chromodynamics*, *Nucl. Phys. B* **189** (1981) 157.
  - [16] M. Di Carlo, G. Martinelli, M. Naviglio, F. Sanfilippo, S. Simula and L. Vittorio, *Unitarity bounds for semileptonic decays in lattice QCD*, *Phys. Rev. D* **104** (2021) 054502 [[2105.02497](#)].
  - [17] L. Lellouch, *Lattice constrained unitarity bounds for anti-B0  $\rightarrow$  pi+ lepton- anti-lepton-neutrino decays*, *Nucl. Phys. B* **479** (1996) 353 [[hep-ph/9509358](#)].
  - [18] A. Gopal and N. Gubernari, *Unitarity bounds with subthreshold and anomalous cuts for b-hadron decays*, *Phys. Rev. D* **111** (2025) L031501 [[2412.04388](#)].
  - [19] N. Gubernari, D. van Dyk and J. Virto, *Non-local matrix elements in  $B_{(s)} \rightarrow \{K^{(*)}, \phi\} \ell^+ \ell^-$* , *JHEP* **02** (2021) 088 [[2011.09813](#)].
  - [20] N. Gubernari, M. Reboud, D. van Dyk and J. Virto, *Improved theory predictions and global analysis of exclusive  $b \rightarrow s \mu^+ \mu^-$  processes*, *JHEP* **09** (2022) 133 [[2206.03797](#)].
  - [21] T. Blake, S. Meinel, M. Rahimi and D. van Dyk, *Dispersive bounds for local form factors in  $\Lambda b \rightarrow \Lambda$  transitions*, *Phys. Rev. D* **108** (2023) 094509 [[2205.06041](#)].
  - [22] J.M. Flynn, A. Jüttner and J.T. Tsang, *Bayesian inference for form-factor fits regulated by unitarity and analyticity*, *JHEP* **12** (2023) 175 [[2303.11285](#)].
  - [23] RBC/UKQCD collaboration, *Exclusive semileptonic  $B_s \rightarrow K \ell \nu$  decays on the lattice*, *Phys. Rev. D* **107** (2023) 114512 [[2303.11280](#)].
  - [24] B. Simon, *Orthogonal polynomials on the unit circle: New results*, *International Mathematics Research Notices* (2004) 2837 [[math/0405111](#)].

- [25] G. Barton, *Introduction to Dispersion Techniques in Field Theory*, Lecture notes and supplements in physics, W.A. Benjamin, New York, Amsterdam (1965).
- [26] I. Caprini, G. Colangelo and H. Leutwyler, *Mass and width of the lowest resonance in QCD*, *Phys. Rev. Lett.* **96** (2006) 132001 [[hep-ph/0512364](#)].
- [27] B. Grinstein and R.F. Lebed, *Above-Threshold Poles in Model-Independent Form Factor Parametrizations*, *Phys. Rev. D* **92** (2015) 116001 [[1509.04847](#)].
- [28] I. Caprini, B. Grinstein and R.F. Lebed, *Model-independent constraints on hadronic form factors with above-threshold poles*, *Phys. Rev. D* **96** (2017) 036015 [[1705.02368](#)].
- [29] E. Fermi and B.T. Feld, *Lectures on pions and nucleons*, *Nuovo Cim.* **2** (1955) 17.
- [30] K.M. Watson, *Some general relations between the photoproduction and scattering of pi mesons*, *Phys. Rev.* **95** (1954) 228.
- [31] M. Kirk, B. Kubis, M. Reboud and D. van Dyk, *A simple parametrisation of the pion form factor*, *Phys. Lett. B* **861** (2025) 139266 [[2410.13764](#)].
- [32] G. Colangelo, M. Hoferichter and P. Stoffer, *Two-pion contribution to hadronic vacuum polarization*, *JHEP* **02** (2019) 006 [[1810.00007](#)].
- [33] C. Bourrely, I. Caprini and L. Lellouch, *Model-independent description of  $B \rightarrow \pi l \nu$  decays and a determination of  $-V(ub)$* , *Phys. Rev. D* **79** (2009) 013008 [[0807.2722](#)], [Erratum: *Phys.Rev.D* **82**, 099902 (2010)].
- [34] S.D. Protopopescu, M. Alston-Garnjost, A. Barbaro-Galtieri, S.M. Flatte, J.H. Friedman, T.A. Lasinski et al., *Pi pi Partial Wave Analysis from Reactions  $\pi^+ p \rightarrow \pi^+ \pi^- \Delta^{++}$  and  $\pi^+ p \rightarrow K^+ K^- \Delta^{++}$  at 7.1-GeV/c*, *Phys. Rev. D* **7** (1973) 1279.
- [35] P. Estabrooks and A.D. Martin, *pi pi Phase Shift Analysis Below the K anti-K Threshold*, *Nucl. Phys. B* **79** (1974) 301.
- [36] S. Simula and L. Vittorio, *Dispersive analysis of the experimental data on the electromagnetic form factor of charged pions at spacelike momenta*, *Phys. Rev. D* **108** (2023) 094013 [[2309.02135](#)].
- [37] D. Stamen, D. Hariharan, M. Hoferichter, B. Kubis and P. Stoffer, *Kaon electromagnetic form factors in dispersion theory*, *Eur. Phys. J. C* **82** (2022) 432 [[2202.11106](#)].
- [38] S. Blatnik, J. Stahov and C.B. Lang, *The Isovector Part of the Kaon Form-factor and the Kaon Charge Radii*, *Lett. Nuovo Cim.* **24** (1979) 39.
- [39] J.R. Peláez and A. Rodas, *Dispersive  $\pi K \rightarrow \pi K$  and  $\pi \pi \rightarrow K \bar{K}$  amplitudes from scattering data, threshold parameters, and the lightest strange resonance  $\kappa$  or  $K0^*(700)$* , *Phys. Rept.* **969** (2022) 1 [[2010.11222](#)].
- [40] N. Muskhelishvili, *Singular Integral Equations*, Springer Dordrecht (1958), <https://doi.org/10.1007/978-94-009-9994-7>.
- [41] R. Omnes, *On the Solution of certain singular integral equations of quantum field theory*, *Nuovo Cim.* **8** (1958) 316.
- [42] BABAR collaboration, *Measurement of the spectral function for the  $\tau^- \rightarrow K^- K_S \nu_\tau$  decay*, *Phys. Rev. D* **98** (2018) 032010 [[1806.10280](#)].
- [43] A. Bharucha, T. Feldmann and M. Wick, *Theoretical and Phenomenological Constraints on Form Factors for Radiative and Semi-Leptonic B-Meson Decays*, *JHEP* **09** (2010) 090 [[1004.3249](#)].
- [44] G. Martinelli, S. Simula and L. Vittorio, *Constraints for the semileptonic  $B \rightarrow D^{(*)}$  form factors from lattice QCD simulations of two-point correlation functions*, *Phys. Rev. D* **104** (2021) 094512 [[2105.07851](#)].
- [45] A. Melis, F. Sanfilippo and S. Simula, *Hadronic susceptibilities for b to c transitions from two point correlation functions*, *PoS LATTICE2023* (2024) 243 [[2401.03920](#)].
- [46] J. Harrison,  *$b^-c$  susceptibilities from fully relativistic lattice QCD*, *Phys. Rev. D* **110** (2024) 054506 [[2405.01390](#)].
- [47] G. Martinelli, S. Simula and L. Vittorio, *Exclusive semileptonic  $B \rightarrow \pi \ell \nu_\ell$  and  $B_s \rightarrow K \ell \nu_\ell$  decays through unitarity and lattice QCD*, *JHEP* **08** (2022) 022 [[2202.10285](#)].